R-07-65

Solute transport in coupled inland-coastal water systems

General conceptualisation and application to Forsmark

Jerker Jarsjö, Georgia Destouni, Klas Persson, Carmen Prieto
Department of Physical Geography, Quaternary Geology
Stockholm University

December 2007

Svensk Kärnbränslehantering AB
Swedish Nuclear Fuel
and Waste Management Co
Box 250, SE-101 24 Stockholm
Tel +46 8 459 84 00

ISSN 1402-3091
SKB Rapport R-07-65

Solute transport in coupled inland-coastal water systems

General conceptualisation and application to Forsmark

Jerker Jarsjö, Georgia Destouni, Klas Persson, Carmen Prieto
Department of Physical Geography, Quaternary Geology
Stockholm University

December 2007

Abstract

We formulate a general theoretical conceptualisation of solute transport from inland sources to downstream recipients, considering main recipient load contributions from all different nutrient and pollutant sources that may exist within any catchment. Since the conceptualisation is model-independent, its main hydrological factors and mass delivery factors can be quantified on the basis of inputs to and outputs from any considered analytical or numerical model. Some of the conceptually considered source contribution and transport pathway combinations are however commonly neglected in catchment-scale solute transport and attenuation modelling, in particular those related to subsurface sources, diffuse sources at the land surface and direct groundwater transport into the recipient. The conceptual framework provides a possible tool for clarification of underlying and often implicit model assumptions, which can be useful for e.g. inter-model comparisons in SKB's site investigation or safety assessment programmes.

In order to further clarify and explain research questions that may be of particular importance for transport pathways from deep groundwater surrounding a repository, we concretise and interpret some selected transport scenarios for model conditions in the Forsmark area. Possible uncertainties in coastal discharge predictions (that underpin all transport results), related to uncertain spatial variation of evapotranspiration within the catchment, were shown to be small for the relatively large, focused surface water discharges from land to sea, because local differences were averaged out along the length of the main water flow paths. In contrast, local flux values within the diffuse groundwater flow field from land to sea are more uncertain, although estimates of mean values and total sums of submarine groundwater discharge (SGD) along some considerable coastline length may be robust. The present results show that 80% to 90% of the total coastal discharge of Forsmark occurred through focused flows in visible streams, whereas the remaining 10% to 20% was diffuse and occurring through submarine groundwater discharge (SGD), small transient streams and/or coastal wetlands.

Regarding transport quantifications, hydrogeochemical characteristics and pollution source loads may generally differ between larger, monitored catchments and smaller unmonitored coastal catchments. Since national hydrological monitoring data systematically exclude smaller, coastal catchments, they may not be representative for conditions in Forsmark (or Laxemar-Simpevarp). This emphasises the importance of extending in time the recently started hydrological and hydrogeochemical data series in the Forsmark and Laxemar-Simpevarp coastal catchment areas, since they are in effect unmonitored from a hydrological viewpoint, due to the lack of extended discharge time series.

In the performed initial demonstration analysis of solute transport pathways from deep groundwater to recipients at the surface, we considered the main scenarios: (I) transport in the Quaternary deposits-bedrock interface zone only (assuming that the deep groundwater transport pathway to the coast excludes the inland surface water system), and (II) transport in the coupled groundwater-surface water system. Considering mean travel times from each model cell to the coast, and disregarding travel times in the deep bedrock domain itself (which may be added to the here presented values), results show that travel times in scenario (II) were less than 4 years in 90% of the considered model area (i.e. the Forsmark catchment area). Travel times were longer in scenario (I) with values higher than 10 years in 40% of the catchment area. These results are based on the assumption that the pathways do not go through zones of near-stagnant groundwater (found e.g. below Lake Bolundsfjärden, Lake Eckarfjärden and Lake Gällsboträsket in Forsmark). If they would do so (and the above assumption is violated), results show that travel times can be considerably longer, for instance exceeding 400 years in half of the model area in scenario (I).

Considering possible solute attenuation (caused by e.g. biogeochemical reactions or decay) along the hydrological transport pathways to inland surface waters and to the coast, we estimate solute mass delivery factors, representing the fraction of mass released in a cell that reaches the considered recipient. Results showed that average delivery factors, representing the whole catchment and equalling expected delivery factors in the probabilistic case, can exhibit considerable differences between transport pathway scenarios (I) and (II). However, the magnitude of the differences in average delivery factors (between transport pathway scenarios as well as between considered release points) depends on the actual attenuation rates (i.e. λ-values). This is because for low λ (for Forsmark: $\lambda < 0.01$ year^{-1}), practically all mass reaches the coast regardless of release point and scenario, and for high λ (for Forsmark: $\lambda > 10$ year^{-1}) only a small fraction of the mass reaches the coast regardless of release point and scenario.

The above results imply that, in general, mass delivery factors to recipients are sensitive to both pathways and entrance points or areas in the Quaternary deposits of Forsmark, with for instance a remaining key question being to which extent the deep groundwater transport pathway to the coast includes the surface water system and/or Quaternary deposits-bedrock interface zone. However, given more specific sub-catchment areas (e.g. of biosphere objects of interest) and possible ranges of attenuation rates (of compounds of interest) from parallel studies, the present analyses also show that robust predictions regarding e.g. mass delivery can in some cases be obtained despite considerable pathway and entrance point uncertainties. Because such cases then can be excluded from further investigation, it appears that specific transport analyses that consider relevant combinations of possible release points, transport pathway scenarios and attenuation rates can be used for delimiting specific priority regions, where remaining uncertainties are high and further experimental investigations and/or monitoring hence may be needed to reduce the uncertainties.

Sammanfattning

Vi formulerar en generell teoretisk konceptualisering av vattenburna ämnens transport från inlandskällor till recepienter. Konceptualiseringen beaktar bidragen till recipienters totala föroreningsbelastning från alla föroreningskällor som kan förekomma inom avrinningsområden. Eftersom konceptualiseringen är modelloberoende, kan dess huvudsakliga hydrologiska parametrar och massleveransfaktorer (ENG: *mass delivery factors*) kvantifieras på basis av indata från vilken analytisk eller numerisk modell som helst.

Några av de konceptuellt behandlade källfördelnings- och transportvägskombinationerna är vanligen försummade i transport- och attenueringsmodellering (med attenuering avses här massflödesminskning i vattnets flödesriktning, utöver eventuell koncentrationsminskning på grund av omblandning) på avrinningsområdesskalan. Speciellt försummas ofta källor i marken, diffusa källor på markytan och direkt grundvattentransport till recepienten. Det konceptuella ramverket ger ett möjligt verktyg för att klargöra underliggande och ofta implicita modellantaganden, vilket kan vara användbart för tex modelljämförelser i SKBs program för platsundersökningar och säkerhetsanalys.

För att ytterligare tydliggöra och förklara forskningsfrågor som kan vara av speciell betydelse för transportvägar från det djupa grundvatten som omger ett förvar, konkretiserar vi och tolkar utvalda transportscenarier i en modell av Forsmarksområdet. Möjliga osäkerheter i modellberäknat vattenutflöde till kusten (som utgör en grund för alla transportresultat), relaterade till osäkerheter i evapotranspirationens rumsliga variation inom avrinningsområdet, visades vara små för de relativt stora, fokuserade ytvattenflödena från land till hav, eftersom lokala skillnader jämnades ut längs vattnets huvudflödesvägar. Däremot är storleken på de lokala diffusa kustutflödena genom grundvattnet osäkrare, fastän beräknade medel-och totalgrundvattenutflöden genom havsbotten (ENG: *submarine groundwater discharge*; SGD) kan vara robusta om man beaktar betydande kuststräckor. De aktuella resultaten visar att 80 % till 90 % av Forsmarksområdets totala kustutflöde sker genom observerbara vattendrag, medan återstående 10 % till 20 % var diffust och sker genom SGD, små tillfälliga vattendrag och/eller kustnära våtmarker.

En svårighet med transportkvantifieringar är att det generellt kan finnas skillnader i hydrogeokemi och föroreningskällors belastning mellan större, övervakade avrinningsområden och mindre, oövervakade kustnära avrinningsområden. Eftersom nationella, hydrologiska övervakningsdata systematiskt exkluderar mindre, kustnära avrinningsområden är det möjligt att de inte är representativa för Forsmark (eller Laxemar-Simpevarp). Detta betonar vikten av att tidsmässigt utöka de nyligen startade hydrologiska och hydrogeokemiska dataserierna i de kustnära avrinningsområdena vid Forsmark och Laxemar-Simpevarp, eftersom områdena, på grund av avsaknaden av tillräckligt långa tidsserier, än så länge måste betraktas som oövervakade i ett hydrologiskt perspektiv.

I den utförda analysen av vattenburna ämnens transportvägar från djupt grundvatten till recipienter vid markytan beaktade vi huvudscenarierna: (I) transport endast i gränsskiktszonen kvartära avlagringar-bergyta (under antagande att det djupa grundvattnets transportväg till kusten exluderar inlandets ytvattensystem), och (II) transport i det sammankopplade grundvatten-ytvattensystemet. Vad gäller medeltransporttider från varje cell i modellen till kusten, om man bortser från transporttider i själva djupbergsdomänen (vilka kan adderas till de värden som presenteras här), visar resultaten att transporttiderna i scenarie (II) var mindre än 4 år i 90 % av det beaktade modellområdet. Transportiderna var längre i scenarie (I) med värden högre än 10 år i 40 % av modellområdet. Dessa resultat baseras på antagandet att transportvägarna inte går genom zoner av nära nog stagnant grundvatten (som rapporterats förekomma tex under Bolundsfjärden, Eckarfjärden och Gällsboträsket i Forsmark). Om de skulle göra det (och antagandet ovan inte gäller), visar resultaten att transporttiderna kan vara väsentligt längre, tex mer än 400 år i halva modellområdet för scenarie (I).

Angående möjlig attenuering av de vattenburna ämnena, orsakad av biogeokemiska reaktioner eller sönderfall, längs de hydrologiska transportvägarna till inlandets ytvatten och till kusten, beräknar vi här massleveransfaktorer vilka kvantifierar fraktionen som når den beaktade recepienten, av den massa som släpps ut i en cell. Resultaten visade att massleveransfaktorernas medelvärde, som representerar hela avrinningsområdet och är lika med den förväntade massleveransfaktorn i det probabilistiska (sannolikhetsbaserade) fallet, kan visa en betydande variation mellan transportvägsscenarierna (I) och (II). Dock berodde avvikelsernas storlek (vad gäller massleveransfaktorernas medelvärde, mellan transportvägsscenarierna såväl som mellan beaktade utsläppspunkter) på den fakiska attenueringshastigheten (dvs λ-värdet). Anledningen är att vid låga λ (för Forsmark: $\lambda < 0.01$ år^{-1}) når praktiskt taget all utsläppt massa kusten, oavsett utsläppspunkt och scenarie, och vid höga λ (för Forsmark: $\lambda > 10$ år^{-1}) når bara en liten fraktion kusten oavsett utsläppspunkt och scenarie.

Resultaten ovan innebär att massleveransfaktorer till recepienter generellt sett är känsliga både för antagna transportvägar och inträdespunkter (eller inträdesareor) till Forsmarks kvartäravlagringar. En återstående nyckelfråga är tex till vilken grad det djupa grundvattnets transportvägar till kusten inkluderar inlandets ytvattensystem och/eller gränsskikstzonen kvartära avlagringar-bergyta. Givet mer begränsade delavrinningsområden, som tex innefattar biosfärsobjekt av intresse, och intervall för möjliga attenueringshastigheter för ämnen av intresse, visar den aktuella analysen dock att robusta modellberäkningar av tex massleverans kan erhållas i vissa fall, trots avsevärda osäkerheter i transportväg och inträdespunkt. Eftersom sådana fall kan avskrivas från ytterligare studier, framstår det som att specifika transportanalyser som tar hänsyn till relevanta kombinationer av möjliga utsläppspunkter, transportvägsscenarier och attenueringshastigheter kan användas för att avgränsa specifika högprioriterade regioner där de återstående osäkerheterna är stora och ytterligare experimentella undersökningar och/eller övervakning kan behövas för att minska osäkerheterna.

Contents

1 Introduction

Contaminant transport quantifications traditionally rely on separate groundwater and surface water system modelling, monitoring and experimentation studies by researchers from often separated hydrogeological and surface hydrological disciplines. The focus of discipline-specific pollutant spreading studies is further limited to either the chemical process details, or the hydro(geo)logical transport details. In particular, the chemical process studies often use oversimplified lumped box/reservoir representations of hydro(geo)logical transport, and the hydro(geo)logical transport studies often use oversimplified chemical reaction descriptions. Large-scale biogeochemical model descriptions may in turn greatly and erroneously simplify or neglect both transport and chemical process details and variability.

SKB performs site investigations at Forsmark, e.g. /Lindborg 2005/, and Laxemar-Simpevarp (Oskarshamn), e.g. /Lindborg 2006/, as a part of the process to find a suitable location for a deep repository for spent nuclear fuel. In case of a repository failure, radionuclides may be released into the deep groundwater surrounding the repository. Deep groundwater is an integrated part of the hydrological cycle and can transport substances (solutes, tracers, colloids and gases) from the proposed future repository depth (about 500 m below the sea surface level) into shallow water systems and the sea, where the substances can potentially affect humans and various biosphere ecosystems.

Hence, in order to understand the consequences of a repository failure, hydrogeological and hydrological primary data and model results are needed as input to ecosystem and safety assessment models, see also /Lindborg et al. 2006, Werner et al. 2006ab, Avila et al. 2006/. Information is for instance needed regarding transport times, locations of surface water and shallow groundwater systems that can be affected by a repository failure, and concentrations in, and total mass flows into, the affected systems. A key task is therefore to develop a site-specific understanding of solute transport processes in coupled groundwater-surface water-coastal water systems. The main aim of this work is to contribute to the development of such a site-specific understanding by proposing a common, general theoretical basis, combining a wide range of recent model- and process-understanding and observation gap quantification results, as further detailed in the following paragraphs.

The transport pathways from the deep groundwater surrounding a repository will have to pass a number of different interfacing hydrogeological and hydrological systems. Such a series of interfaces can generally disperse solutes travelling through the whole zone. In addition, traditional hydrogeological model boundaries, such as the lower boundary of shallow groundwater models, or the upper boundary of deep groundwater models, intersect and cut through the interfacing hydrogeological systems in different ways. Therefore, their characteristics are often not very well represented in such models, even if they are coupled.

The models may, for instance, neglect the dispersive nature of hydrogeological system interfaces. As a consequence, they may fail to reproduce potentially important environmental effects of source zones in deep groundwater. For instance, due to dispersion over system interfaces, a point source in deep groundwater may influence surface and coastal water systems in a similar way as a diffuse source in shallow groundwater. This means that the solute may spread over a large part of the waters and ecosystems at the surface, even if such dispersion also may decrease solute concentrations in some areas. It is therefore a great challenge to find a relevant and consistent process detail and complexity level in the large spatial-temporal model scales involved in pollutant spreading along integrated ground-surface-coastal water and solute pathways.

In a series of concerted recent studies, we have found considerable regional to worldwide gaps in available observation and monitoring data of waterborne tracer, nutrient and pollutant loads /Destouni and Gren 2005, Hannerz and Destouni 2006, Destouni et al. 2008/. These

gaps limit our process understanding and prohibit sufficient critical model testing against observations. This is most striking for subsurface processes of waterborne tracer, nutrient and pollutant transport and attenuation /Baresel and Destouni 2005, Destouni et al. 2008/.

In another series of recent studies, we found also that such gaps in our process understanding and model testing possibilities have allowed important model differences and scientific disagreement to prevail. At least, this is the case regarding the relevant model representation of waterborne tracer, nutrient and pollutant transport and attenuation processes in inland water catchments and from land to sea /Lindgren and Destouni 2004, Darracq and Destouni 2005, Destouni and Darracq 2006, Destouni et al. 2008/. Hence, commonly used investigation and modelling methods may fail to give realistic explanatory and predictive descriptions of the large-scale cause-effect relations in the coupled ground-surface-coastal water system that link subsurface pollutant sources with downstream waters, as detailed through several studies /Malmström et al. 2000, Kavanaugh et al. 2003, Destouni and Prieto 2003, Malmström et al. 2004, Lindgren and Destouni 2004, Jarsjö et al. 2005, Darracq and Destouni 2005, Prieto and Destouni 2005, Bayer-Raich et al. 2006, Malmström et al. 2008/.

There is now a need to bridge these observation and process understanding gaps, and resolve disagreements about appropriate process modelling among numerous available but importantly differing models of the waterborne transport and attenuation of different substances (see, e.g. model reviews and comparisons by /Kavanaugh et al. 2003, Darracq and Destouni 2005, Destouni et al. 2008/). As a first step, we here provide a common, general theoretical conceptualisation and quantification basis that can facilitate direct and consistent comparison and testing against observation data of the input, output and calibration results of different used models. Further, we review current knowledge regarding groundwater discharges into rivers, lakes and the sea. These discharges can be considerable and hence important for solute transport, but the knowledge about them is critically limited by measurement/estimation difficulties. Finally, we use the developed framework for performing an initial demonstration analysis of solute transport along different possible pathways through coupled ground-surface-coastal water systems of Forsmark, identifying also key issues to be addressed for obtaining an increased site-specific understanding of such transport.

2 Transport processes and pathways

2.1 Background: Processes at the local scale

(Bio)degradation rates, attenuation rates and sorption characteristics may exhibit considerable spatial variation within coupled subsurface-surface systems. At the catchment scale, solute mass delivery into recipients from contaminant source zones may therefore largely depend on the physical location of the transport pathways between the source zones and the recipients, as further explained and addressed in section 2.2. However, more locally, at length scales around or below 50 metres, effective degradation rates, representative for the local subsurface and surface systems, have been estimated through field observations. Such field-determined degradation rates may differ considerably from those determined in the laboratory. This is not least the case for biodegrading contaminants, such as petroleum products (hydrocarbons). The reason is that the biogeochemical characteristics of, in particular, the subsurface system is difficult to reproduce in the laboratory.

These field-measured attenuation and degradation rates are back-calculated from either concentration changes detected along an estimated plume core or centreline, or concentration or mass flow changes detected over consecutive control planes (CPs) perpendicular to the main flow direction, at different downstream distances from the contaminant source. Recent studies have however shown that such back-calculated degradation rates may be associated with considerable uncertainty, e.g. /Bauer et al. 2006, Li et al. 2007, Jarsjö et al. 2008/, unless the local flow directions and mass flows are determined with relatively high accuracy. For instance, /Jarsjö et al. 2008/ showed that a mass flow estimation error of 20% or less can propagate and cause order-of-magnitude errors in back-calculated degradation rates, which partly can explain the large differences in reported degradation rates of field studies.

In principle, with the exception of radioactive decay, degradation of a compound may in a porous medium take place at different rates depending on if it is dissolved in the aqueous phase or sorbed onto the solid phase. Therefore, theoretical studies often distinguish between λ_w [T^{-1}], the degradation rate in the aqueous phase and λ_s[T^{-1}], the degradation rate in the solid phase. Due to measurement difficulties, such distinctions have not been made in experimental studies that consider field conditions. Instead, a relatively large number of studies, e. g. /Buscheck and Alcantar, 1995, Konikow et al. 1996, Wiedemeier et al. 1999, Quezada et al. 2004, Falta et al. 2005/ are based on the following assumptions:

(a) "degradation takes place only in the aqueous phase at rate λ_a", which then specifically implies that $\lambda_a = \lambda_w$ and $\lambda_s = 0$, or

(b) "degradation takes place in both aqueous and solid phases at the same rate λ_b", which then specifically implies that $\lambda_b = \lambda_w = \lambda_s$.

The above degradation-assumptions can be compared with two commonly used assumptions regarding retardation namely:

(c) "steady-state solutions are independent of the retardation factor R",

(d) "linear retardation is accounted for by dividing the water velocity by a factor R".

with the retardation factor R defined as $R = 1 + \rho_b K_f / n_e$, where ρ_b [M L^{-3}] is the soil bulk density, K_f [L^3 M^{-1}] is an empirical distribution coefficient and n_e is the effective porosity. We note that both assumptions (c) and (d) are simultaneously true and generally valid when considering the advection-dispersion-retardation transport without degradation. Now, if degradation is also accounted for, assumption (c) is true only in settings where assumption (a) is applicable, and assumption (d) is true only in settings where assumption (b) is applicable.

However, above simplifying assumptions (a) to (d), for which open research questions remain regarding their applicability at larger scales, are actually not required when considering linear sorption and first order degradation at larger scales. This is because there is an alternative and less restrictive interpretation of λ-values obtained from observed concentration and mass flow changes over consecutive control planes (CPs) in the field. Specifically, such λ-values should be viewed as "effective" values, which reflect weighted proportions of (potentially different) degradation rates in the solid (λ_s) and aqueous phases (λ_w). For instance, such a weighting relation is

$$\lambda = (1/R)\lambda_w + ((R-1)/R)\lambda_s \qquad \text{Equation 2.1}$$

in which λ then is considered to be a weighted average of actual λ´s in the soil and water phases (λ_w and λ_s), where the weighting factors $(1/R)$ and $((R-1)/R)$ can be interpreted as the time that the contaminant spends moving through the aqueous phase and immobilized in sorbed phase, respectively. This means that during an increment of time Δt a particle of contaminant moving through the aquifer will spend $(1/R)\Delta t$ units of time moving through the aqueous phase and $((R-1)/R)\Delta t$ units of time immobilized in the sorbed phase.

2.2 The catchment scale

2.2.1 Novel, general theoretical conceptualisation

Retardation and attenuation of dissolved nutrients, organic compounds, hydrocarbons, trace elements and radionuclides are governed by physical, chemical and hydrogeological conditions that can differ considerably within and between groundwater, (inland) surface water and coastal water systems. This implies that the contaminant pathway, and in particular whether or not the transport path intersects specific characteristic water systems (illustrated schematically in Figure 2-1), considerably influence the relation between the total mass flows emitted by inland contaminant sources (filled red circles in Figure 2-1) and the total contaminant mass flows (loads) reaching the coastal water systems. For transport from an inland source to the coast, the dominating path may either be through the coupled groundwater-stream system (thick arrow

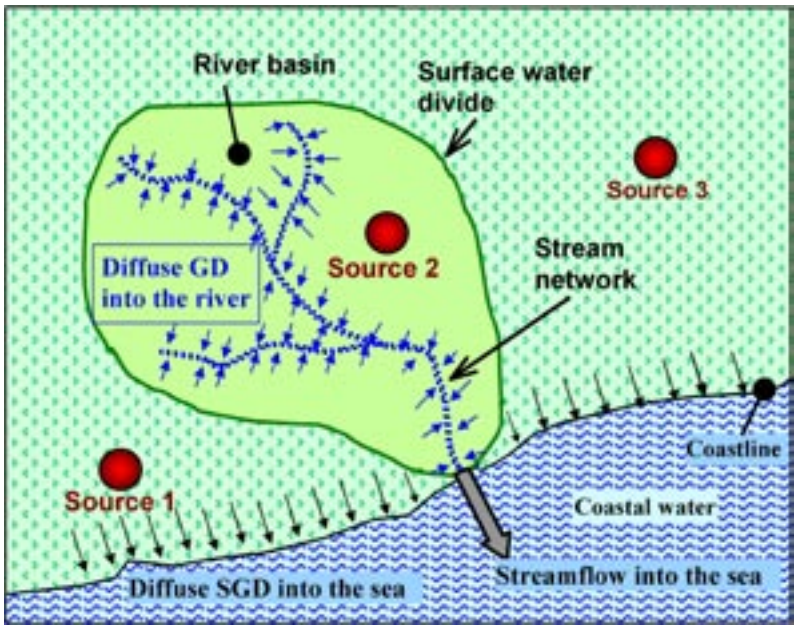

Figure 2-1. *Schematic view showing how groundwater provides a link between contaminant sources (filled red circles) and the sea, through groundwater discharge (GD) into rivers, and submarine groundwater discharge (SGD) into the sea.*

at the river basin outlet in Figure 2-1, including the contribution of the diffuse groundwater discharge into the river, illustrated by the thin blue arrows) or through direct groundwater discharges to coastal waters (thin black arrows in Figure 2-1).

The knowledge about the magnitude of these direct groundwater discharges is critically limited by measurement/estimation difficulties. However, it is generally recognised that they can constitute a considerable part of the total freshwater outflow to the sea (illustrated by the thin black arrows in Figure 2-1), with some studies even showing magnitudes similar to the contribution by streams and rivers /Moore 1996, Li et al. 1999/ (thick arrow at the basin outlet in Figure 2-1). It is further recognised that such groundwater discharges are chemically and ecologically important to coastal waters, see further /Moore 1999/ and review by /Burnett et al. 2003/.

We here consider continuous mass release under steady-state conditions and refer to /Lindgren and Destouni 2004/ for other expressions relevant for e.g. pulse releases. The mean nutrient/pollutant mass flow, or periodically cumulative mass load (e.g. mean annual integral of mass flow rate), denoted here S_r^{tot}, from all the catchment areas *i* that may contribute a mass load into a downstream water recipient *r* (lake, stream, river, or coastal water; or if remaining in the subsurface water system a groundwater supply area or well field) may then be expressed as:

$$S_r^{tot} = \sum_i S_r^i \qquad \text{Equation 2.2}$$

The mean nutrient/pollutant mass flow or periodically cumulative mass load, S_r^i, from each catchment area *i* into the recipient *r* includes load components from all different nutrient and pollutant sources within the catchment area. These components may be grouped as:

$$S_r^i = [\sum_j S_{s-out}^{p,j} + \sum_k S_{sf-out}^{d/p,k} + \sum_m S_{ss-out}^{d/p,m}]^i \qquad \text{Equation 2.3}$$

including recipient load contributions: $S_{s-out}^{p,j}$ from all point source emissions $S_{s-in}^{p,j}$ directly into streams; $S_{sf-out}^{d/p,k}$ from all diffuse and/or point source mass inputs $S_{sf-in}^{d/p,k}$ on the surface; and $S_{ss-out}^{d/p,m}$ from all diffuse and/or point source mass inputs $S_{ss-in}^{d/p,m}$ in the subsurface. Figure 2-2a shows an example of a point source in the subsurface, which would yield a mass flow of $S_r^{tot} = S_{ss-out}^{p}$ into the recipient lake in absence of other sources. Figure 2-2b further shows an example of a point source on the surface, which would yield a mass flow of $S_r^{tot} = S_{sf-out}^{p}$ into the recipient lake in absence of other sources. As previously indicated, solute attenuation generally implies that S_r^{tot} is smaller than the sum of mass flow inputs from all contaminant sources. We will in the following further clarify the relation between the mass flow input, possible transport pathways, attenuation-decay along the possible pathways, and the resulting mass flows into considered recipients.

The reason for grouping the recipient load components as in Equation 2.3 is that they represent the main, distinctly different spatial configuration types of possible source and pathway-to-recipient combinations within any catchment. Such spatially related grouping has already been found useful for identifying, classifying and quantifying main discrepancies between and associated uncertainties in different catchment-scale nutrient transport-attenuation models /Destouni et al. 2008/. Each of the main recipient load components in Equation 2.3 may then without loss of generality be expressed as:

$$S_{s-out}^{p,j} = S_{s-in}^{p,j} \alpha_s^{p,j} \qquad \text{Equation 2.4a}$$

$$S_{sf-out}^{d/p,k} = S_{sf-in}^{d/p,k} (\beta_{gw}^{k} \gamma_{gw-s}^{k} \alpha_{gw-s}^{d/p,k} + (1-\beta_{gw}^{k}) \alpha_s^{d/p,k} + \beta_{gw}^{k} (1-\gamma_{gw-s}^{k}) \alpha_{gw}^{d/p,k}) \qquad \text{Equation 2.4b}$$

$$S_{ss-out}^{d/p,m} = S_{ss-in}^{d/p,m} (\gamma_{gw-s}^{m} \alpha_{gw-s}^{d/p,m} + (1-\gamma_{gw-s}^{m}) \alpha_{gw}^{d/p,m}) \qquad \text{Equation 2.4c}$$

The quantity $0 \leq \beta_{gw} \leq 1$ is the fraction of total effective precipitation (precipitation minus evapotranspiration) that infiltrates the soil and recharges groundwater, while γ_{gw-s} quantifies the fraction of that subsurface recharge that contributes to stream flow within the catchment area *i*. These quantities may be characteristic hydrological factors or functions for the whole catchment area *i*, or spatially dependent on the subareas associated with the different diffuse or point sources *k,m* within the catchment. The complementary factor or function $(1-\beta_{gw})$ quantifies the remaining fraction of total effective precipitation that directly yields stream flow without flowing through the soil-groundwater system, and $(1-\gamma_{gw-s})$ quantifies the fraction of subsurface water recharge that flows into the recipient (or downstream sub-catchment) as groundwater without contributing to stream flow within the catchment area *i*.

Finally, the various $0 \leq \alpha \leq 1$ factors or functions in Equation 2.4 quantify the resulting relative nutrient/pollutant mass delivery into the recipient from any diffuse or point source mass input and subsequent waterborne mass transport and attenuation through only the stream network (α sub-index *s*), or through only the subsurface soil-groundwater system (α sub-index *gw*), or through both the soil-groundwater and the stream network system (α sub-index *gw–s*). The complementary quantities $(1-\alpha)$ quantify both irreversible and long-term (i.e. longer than any periodic time-integration of S_r^i) reversible attenuation of nutrient/pollutant mass fraction in each system.

Table 2-1 lists and explains the various combinations and physical meaning of the different source, transport-attenuation and delivery pathway terms that are included in the Equation 2.4a–c components. These terms are generally composed of two main hydrological (β_{gw} and γ_{gw-s}) and two main mass delivery ($\alpha_s^{d/p}$ and $\alpha_{gw}^{d/p}$) factors or functions (with the $\alpha_{gw-s}^{d/p}$ term in Equations 2.4b–c being products of these factors/functions, as $\alpha_{gw-s}^{d/p} = \alpha_{gw}^{d/p}\alpha_s^{d/p}$) that represent the water flow and waterborne mass transport and attenuation processes that govern any catchment area's nutrient and pollutant loading to its recipient.

Table 2-1. Combinations and physical meaning of the different source, transport-attenuation and delivery pathway terms included in Equation 2.4a–c.

Spatial source configuration	Transport pathway					
	Through soil-groundwater to stream network to recipient		Through the stream network to recipient		Through soil-groundwater to recipient	
	Relative mass input	Relative mass output	Relative mass input	Relative mass output	Relative mass input	Relative mass output
Point source input $S_{s-in}^{p,j}$ directly into streams yielding total recipient load $S_{s-out}^{p,j}$ Equation 2.4a	---	---	1	$\alpha_s^{p,j}$	---	---
Diffuse or point source mass input $S_{sf-in}^{d/p,k}$ on land surface yielding total recipient load $S_{sf-out}^{d/p,k}$ Equation 2.4b	$\beta_{gw}^k \gamma_{gw-s}^k$ ----------	$\alpha_{gw-s}^{d/p,k} = \alpha_{gw}^{d,k}\alpha_s^{d,k}$	$(1-\beta_{gw}^k)$	$\alpha_s^{d/p,k}$	$(1-\gamma_{gw-s}^k)$ ----------	$\alpha_{gw}^{d/p,k}$ ---------
Diffuse or point source mass input $S_{ss-in}^{d/p,m}$ in the subsurface yielding total recipient load $S_{ss-out}^{d/p,m}$ Equation 2.4c	γ_{gw-s}^m ----------	$\alpha_{gw-s}^{d/p,m} = \alpha_{gw}^{d,m}\alpha_s^{d,m}$ ----------	---	---	$(1-\gamma_{gw-s}^m)$ ----------	$\alpha_{gw}^{d/p,m}$ ---------

Figure 2-2 further illustrates which components of Equations 2.4a–c that are relevant for which contaminant pathways. Figure 2-2a shows pathways from a subsurface point source (green filled circle in Figure 2-2) to a recipient lake (dark blue in Figure 2-2) through groundwater only (red dotted line in Figure 2-2a; Equation 2.4c component $(1-\gamma_{gw-s})\alpha^{p}_{gw}$), and a pathway through the coupled groundwater – surface water system (orange continuation of the red dotted lines in Figure 2-2a; Equation 2.4c component $\gamma_{gw-s}\alpha^{p}_{gw-s}$; the surface water system is shown in light blue colour). Figure 2-2b shows pathways from a point source at the ground surface to a recipient lake through groundwater only (red dotted line in Figure 2-2b; Equation 2.4b component $\beta_{gw}(1-\gamma_{gw-s})\alpha^{p}_{gw}$), a pathway through the coupled groundwater-surface water system (orange dotted lines in Figure 2-2b; Equation 2.4b component $\beta_{gw}\gamma_{gw-s}\alpha^{p}_{gw-s}$), and a pathway through the surface water system (yellow dotted line in Figure 3; Equation 2.4b component $(1-\beta_{gw})\alpha^{p}_{s}$).

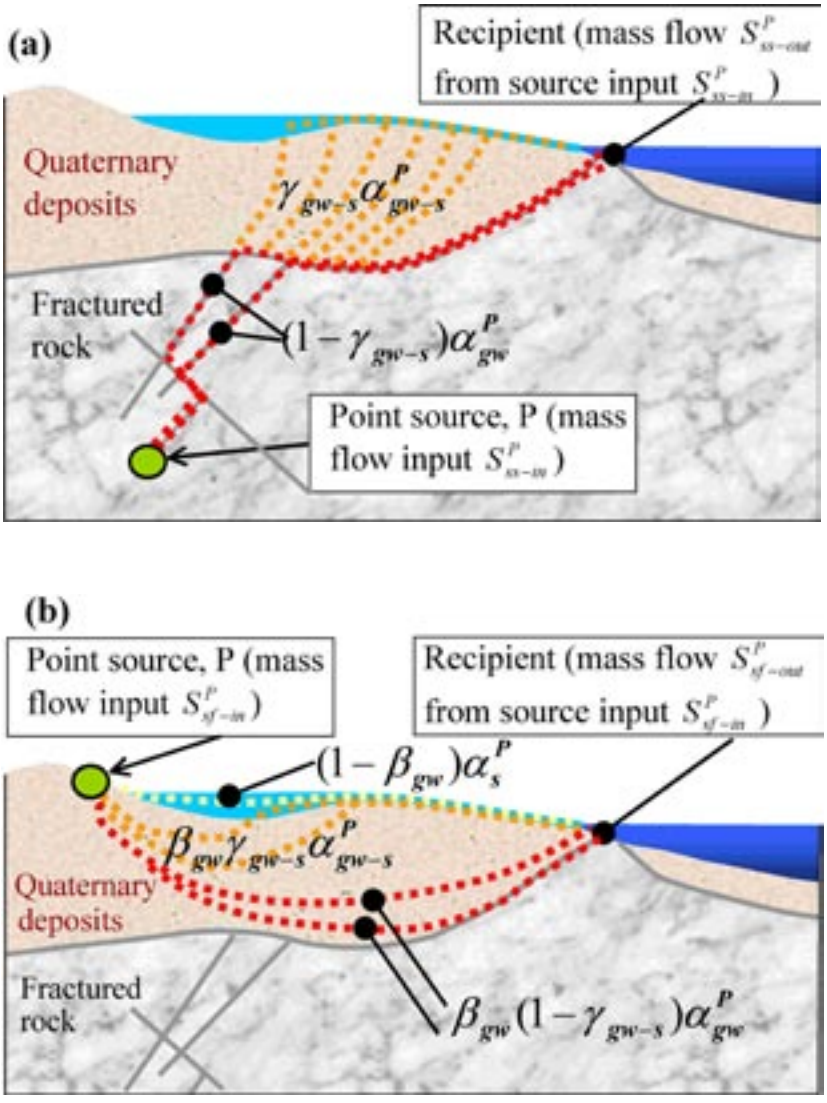

Figure 2-2. *Example illustration of possible solute transport paths to a receptor (a) from a point source in the subsurface (red, dotted line: path through the groundwater (gw) system; orange, dotted line: path through the coupled groundwater – surface water (gw–s) system) and (b) from a point source on the surface (yellow, dotted line: path through the surface water (s) system; orange, dotted line: path through the gw–s system; red line: path through the gw system).*

2.2.2 Using the framework as a quantification basis

Given the setting of continuous mass release under steady-state conditions, Equations 2.4a–c are general, i.e. valid for both linear and non-linear attenuation processes, and model-independent. This means that any coupled hydrological and waterborne nutrient/pollutant transport and attenuation model may be used for site-, source-pathway- and scenario-specific quantification of its main hydrological factors (β_{gw}, and γ_{gw-s}), and mass delivery factors ($\alpha_s^{d/p}$ and $\alpha_{gw}^{d/p}$). Such quantification can be performed on the basis of inputs to and outputs from the model, either analytically or numerically (depending on the model used). Consistent summary of the input-output data and calibration parameters of different models in terms of resulting β_{gw}, γ_{gw-s}, $\alpha_s^{d/p}$ and $\alpha_{gw}^{d/p}$ factor/function quantification facilitates direct comparison between the essential implications of and differences between underlying model assumptions, process representations and results. Such comparison facilitates in turn also identification of possible general essential uncertainty components in modelling that need to be bridged by concerted observation, monitoring and modelling improvement efforts.

An example analytical model for such quantification may be expressed as

$$\beta_{gw} = A_{sw}/A_{catch} \qquad \text{Equation 2.5a}$$

$$\gamma_{gw-s} = Q_{sw}/Q_{tot} \qquad \text{Equation 2.5b}$$

$$\alpha_s^{d/p} = \int_0^{\infty} \exp[-\lambda_s \tau_s] f_s(\tau_s) d\tau_s \qquad \text{Equation 2.5c}$$

$$\alpha_{gw}^{d/p} = \int_0^{\infty} \exp[-\lambda_{gw} \tau_{gw}] g_{gw}(\tau_{gw}) d\tau_{gw} \qquad \text{Equation 2.5d}$$

where A_{sw} is the area of the surface water system (e.g. streams and lakes) within the catchment, A_{catch} is the catchment area, Q_{sw} is the focused (surface water) discharge from the catchment, Q_{tot} is the total (focused + diffuse) discharge from the catchment, equalling under steady-state conditions the average precipitation surplus times A_{catch}, τ is the travel time, and $f_s(\tau_s)$ and $g_{gw}(\tau_{gw})$ are travel time distributions for the surface water system and groundwater system, respectively; see chapter 5 for example quantifications of these factors for the Forsmark catchment.

Even without any specific model quantification of different terms, their conceptualisation in Equations 2.4a–c and Table 2-1 clarifies directly some commonly neglected components in catchment-scale solute transport and attenuation modelling. These are all the underlined terms in Table 2-1, which are all related to subsurface sources, and the partitioning of mass input and further downstream transport-attenuation of nutrients and pollutants from these sources, and of diffuse sources at the land surface, between the surface waters within the catchment and direct groundwater transport into the recipient. These components are often neglected, because they are difficult to observe and quantify. However, by considering them in the here presented general theoretical framework, their possible contributions to the total contaminant mass loads can be estimated. Such estimates can provide a sound basis for directing field measurement campaigns to areas or zones where they are most needed, e.g. to reduce uncertainty in mass load quantifications.

3 Discharge of groundwater into rivers, lakes and the sea

Groundwater may interact with different types of surface water systems, such as streams, lakes, wetlands and estuaries or the sea. Groundwater interactions with streams, lakes and wetlands are present in nearly all types of landscapes. Useful insights into these natural interactions in five different types of landscapes: riverine, coastal, glacial, dune and karst, are provided by /Winter et al. 1998/ and /Winter 1999/. Lakes in glacial and dune terrains, for instance, can have relatively more complex interactions with groundwater than lakes in other landscapes according to /Winter et al. 1998/. Generally, the interactions of groundwater with surface water bodies are complex and controlled by the topography, the geologic framework and the climatic settings of the landscape /Winter 1999, Sophocleous 2002/. As a consequence, they are subject to high spatial and temporal variability in each landscape.

Theoretically, the interaction between groundwater and a surface water body can take place in several ways: groundwater discharges into surface water systems throughout their entire sediment bed (gaining streams, discharge lakes or wetlands, submarine groundwater discharge), groundwater receives some contribution from surface waters throughout their entire bed (losing streams, recharge lakes or wetlands and submarine groundwater recharge), or do both discharge and recharge the surface water system at different locations. We focus here on the role of groundwater as effluent to surface waters in both the inland water systems and marine environments. The reason is that these discharges constitute the possible transport pathways to the surface and ultimately to the coast of radioactive substances that may be released from deep repositories of nuclear waste stored in the subsurface.

The direct groundwater discharge into the marine environment, commonly called submarine groundwater discharge (SGD), has recently become the focus of relatively many scientific studies, mainly due to the efforts of an international working group on SGD, the SCOR/LOICZ (Scientific Committee on Oceanic Research/Land-Ocean Interaction in the Coastal Zone) working group 112, and a joint project of UNESCO and the IAEA (the International Atomic Energy Agency), see e.g. the review article of /Burnett et al. 2006/. However, although much progress has been made, its global significance, driving forces, spatial distribution and temporal variability are not completely well understood /Burnett et al. 2003, 2006/. On the contrary, the interactions between groundwater and inland water systems such as lakes have been studied since the 1960s /Sophocleous 2002/. In the next sections, we present some reported estimates of groundwater discharge to the marine and the inland water environments, as well as measurement and modelling techniques that are available to quantify and investigate these discharges.

3.1 Groundwater discharge to the sea

It is now recognized that submarine groundwater discharge can be an important pathway for the transport of contaminants to coastal waters /Burnett et al. 2006/. The definition of SGD has been confusing in the literature, but it is now generally agreed /Burnett et al. 2003, 2006/ that the term refers to any flow of water discharging into the sea across continental shelf sediments independently of its composition (fresh, brackish or saline water), origin (terrestrial or marine) or driving forces (terrestrial hydraulic gradient, tides, wave, density or thermal convection). SGD may occur as spring or as diffuse seepage on continental margins involving multiple coastal aquifer-sediment systems: confined, semi-confined and unconfined (Figure 3-1).

Figure 3-1 shows the classical saltwater wedge that develops by seawater intrusion due to the density difference existing between the fresh groundwater in the aquifer and the seawater (STZ in Figure 3-1). Within the saltwater wedge, at least some of the intruding seawater recirculates

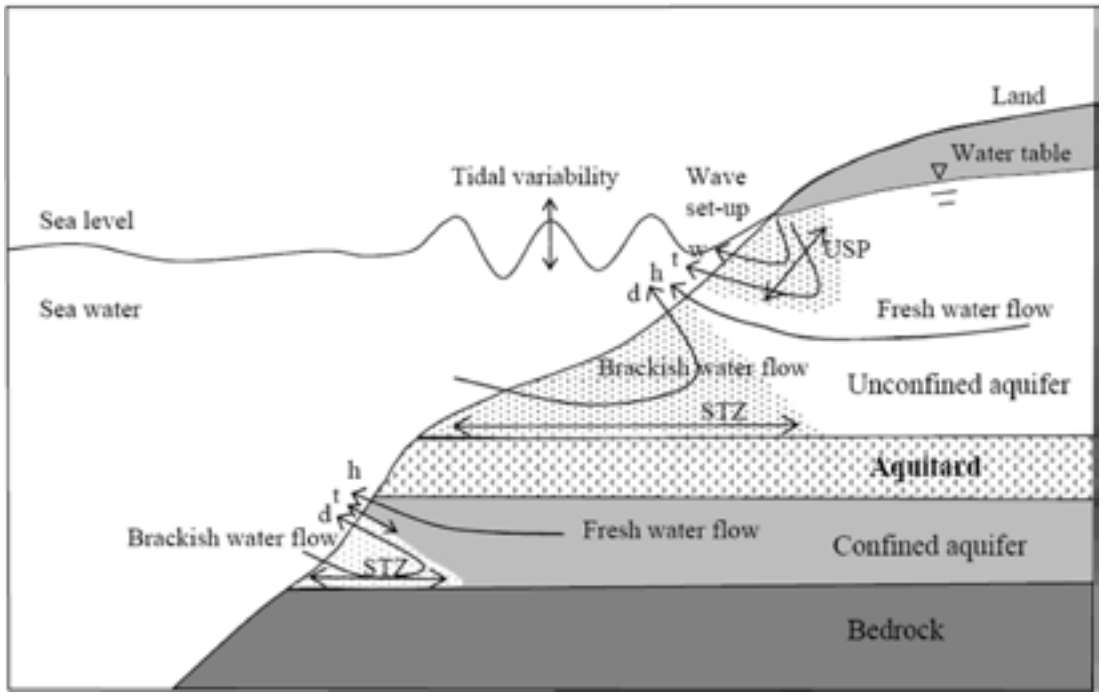

Figure 3-1. *Conceptual cross-section of a multiple coastal aquifer and some SGD components according to the following driving forces: (h) terrestrial hydraulic gradient, (d) density-driven circulation, (t) tidally-driven circulation and (w) wave set-up circulation. STZ refers to the salinity transition zone and USP to the upper salinity plume (after /Taniguchi et al. 2002/ and /Robinson et al. 2007/).*

back into the sea. This flow is at steady-state in dynamic equilibrium with the seaward flow of fresh groundwater that discharges into the sea through the sediments. Recently, /Robinson et al. 2006, 2007/ showed by both field measurements and numerical simulations that in addition to the classical saltwater wedge, near-shore SGD driving forces such as tides and wave set-up may create an upper saline plume (USP in Figure 3-1) in the intertidal region of a sloping beach with salinity values decreasing with aquifer-sediment depths. Seawater recirculates in the upper saline zone in a similar way as in the saltwater wedge but due to different mechanisms. These seawater recirculation areas confine the fresh groundwater flow that discharges near the low tide mark /Robinson 2006, 2007/. It is this terrestrially-derived freshwater portion of total SGD that is of primary concern in case of contamination of groundwater by radioactive substances.

The significance of terrestrially-derived fresh SGD in the global water balance is still not clear. /Burnett et al. 2003/ presents a compilation of several global fresh SGD estimates ranging from 0.3% to 16% of global surface discharge, which is estimated to be equal to 37,400 km^3/yr. These estimates are, however, typically uncertain due to the many different assumptions made in the hydrological calculations, global water balances or hydrograph separation techniques on which they are based. Although /Burnett et al. 2001/ state that the global fresh groundwater discharge is probably no larger than 5% of river discharge, in some areas such as karst regions, SGD may dominate total runoff. It is in fact at the local scale where SGD may be an important process /Burnett et al. 2001/. But, even if the magnitude of the discharge is not relevant in some areas, its ecological impact may be comparatively more significant than the coastal discharge of surface water due to that groundwater has usually higher concentrations of dissolved pollutants than surface waters. As a result, the groundwater contaminant load to the sea may be comparable to or higher than the contaminant river load /Destouni et al. 2008/.

In general, the highest fresh SGD rates tend to be found within a very short distance from the shore (tens to hundreds of meters). However, the terrestrially-derived fresh SGD can discharge up to several tens of kilometers offshore when geological conditions allow it even in siliciclastic

coastal areas /Kooi and Groen 2001/. The exact spatial distribution of total SGD and its fresh and recirculated seawater components along and across a shoreline is, however, highly variable, may change in time and is difficult to evaluate. By a compilation of many different SGD estimates in different parts of the world, /Taniguchi et al. 2002/ showed that SGD was largest at the shoreline and tended to decrease with water depth, i.e. with the distance from the shoreline. In fact, some studies suggest an exponential decrease of SGD rates with the distance from shore /McBride and Pfannkuch 1975, Fukuo and Kaihotsu 1988/. This relationship has, however, been questioned later on by /Bokuniewicz 1992/.

/Taniguchi et al. 2002/ carried out a compilation of all available literature citations where SGD was either mentioned to be significant or was estimated from direct measurements. Most of the compiled observations were concentrated along the east coast of USA, the Mediterranean coastline, Japan and Oceania. In most cases, the reported SGD fluxes were smaller than 36.5 m/yr. Out of over forty compiled SGD observations around the world only two were from the Baltic Sea, in particular along the Southern Baltic Sea coastline. These estimates correspond to 0.15 m/yr in Puck Bay /Piekarek-Jankowska 1996/ (cited in /Taniguchi et al. 2002/) and 75 m/yr in Laholm Bay /Vanek and Lee 1991/ (cited in /Taniguchi et al. 2002/). The relatively large difference in resulting estimates may probably be the result of different geological and coastal conditions such as wave set-up in the studied areas. More recently, SGD measurements were performed at Eckernförde Bay in the western part of the Baltic Sea resulting in a range of 26 to 373 m/yr /Karpen et al. 2006/.

With the main objective of assessing different methodologies for SGD evaluation, the 5-year joint project of UNESCO and IAEA started in 2000 and carried out carefully designed intercomparison experiments in five different hydrogeologic environments (a coastal plain in Australia, karst in Sicily, glacial till in New York, fractured crystalline rock in Brazil, and volcanic terrains in Mauritius) /Burnett et al. 2006/. In all five intercomparison experiments, seepage meters, radium (Ra) and radon (Rn) measurements were used to estimate SGD. Additionally in some case studies, SGD was also estimated using modelling techniques.

The resulting SGD estimates from the different intercomparison experiments except the one performed in the fracture crystalline rock environment in Brazil ranged from 0.4 m^3 day^{-1} (m shoreline)$^{-1}$ at the glacial till or the volcanic terrains sites from seepage meter measurements to 1,000 m^3 day^{-1} (m shoreline)$^{-1}$ at the karst site from radium measurements /Burnett et al. 2006/. It should be noticed that we here report the SGD measurements of the inter-comparison experiments as volume per unit time per meter of shoreline instead of volume per unit time per unit area because the relevant sea floor areas subject to SGD fluxes were not reported in each case. In addition to velocity units and the units of volume per time and meter of shoreline, SGD rates can also be presented in units of volume per unit time. Unfortunately, direct comparisons of SGD rates are not always possible due to differences in reported units and lack of additional information needed for unit conversions. This is the reason why the results from the Brazilian intercomparison experiment could not be compared with the other four field studies.

At each specific intercomparison site, the different applied measurement techniques resulted in different measured SGD ranges. For example, in the glacial till coastal environment, the SGD estimates from seepage meters ranged between 0.4–17.5 m^3 day^{-1} (m shoreline)$^{-1}$, while the SGD results from radon measurements ranged between 8–20 m^3 day^{-1} (m shoreline)$^{-1}$, i.e. they overlapped and were higher than the seepage meters results. Moreover, the radium estimates (16–26 m^3 day^{-1} (m shoreline)$^{-1}$) overlapped the Rn measurements and were generally higher than the radon and seepage meters measurements.

In general, all measurement techniques used in the intercomparison experiments resulted in reasonable estimates, although care should be taken in interpreting Rn and Ra measurements from volcanic aquifers due to that the tracer signal may be weak. The main conclusion of the intercomparison experiments is that SGD is present in any coastal environment and is highly variable in space and time. Therefore, it is recommended to use multiple techniques for its assessment in order to cover the large temporal and spatial scales over which SGD may vary.

3.2 Groundwater discharge to streams and lakes

Groundwater contributes to streams in most topographical, geological and climatic settings /Winter et al. 1998/. However, the proportion of the groundwater contribution to streams varies across different settings. In 24 regions of USA delineated according to distinctive physiographic and climatic settings, the groundwater contribution to streams ranged from 14% to 90% /Winter et al. 1998/. In Sweden, /Grip and Rodhe 2000/ used ^{18}O to investigate the origin of water in stream flow peaks caused by rainfall events, snowmelt episodes and whole spring floods (that often contained several peaks). They reported that most of the stream water during rainfall events, snowmelt episodes and spring floods is derived from groundwater. The groundwater contribution to stream flow ranged from 68 to 100% in the investigated rainfall events, from 32 to 91% in the snow melting episodes and from 41 to 86% during spring floods.

With regard to lakes, the groundwater contribution may generally not be significant relative to the surface water discharge, however, groundwater discharge may play an essential role in the hydrochemical and thermal balance of the lake. For instance, although groundwater discharge only constitutes 0.5% and 1% of the surface water discharge to lake Balkhash in Kazakhstan and to the Caspian Sea, respectively, groundwater carries a significant portion of the salts discharged to them by surface waters (26% and 27% for lake Balkhash and the Caspian Sea, respectively) /Zekster 1996/. Another illustrative example of the groundwater discharge role to lakes is the close-basin Williams lake in Minnesota. In this case, only half of the annual water input to the lake comes from groundwater (the other half from precipitation), but this discharge carries most of the chemical input to the lake /Schuster et al. 2003/.

The groundwater discharged into surface water systems may have the origin in different recharge areas. Therefore, the groundwater flowpaths can have different lengths and corresponding travel times from the recharge areas to the discharge into the surface water system. In Williams lake in Minnesota, for example, the groundwater discharge originates only from the upper part of the surficial aquifer /Schuster et al. 2003/. On the contrary, a study of the groundwater discharge into Utah Lake concluded that the groundwater originated from deep confined aquifers /Zekster 1996/. Furthermore, the origin of the discharged groundwater could be within the delineated surface watershed or outside the surface watershed boundaries. A review of different field studies presented by /Winter et al. 2003/ reveals that certain lakes and wetlands in the small watersheds of Wisconsin, Minnesota and Nebraska receive groundwater inflow from shallow flow systems that extend far beyond their surface watershed, and that they may also receive groundwater inflow from deeper regional flow systems that pass at depth beneath local flow systems.

Similarly, at the La Selva Biological Station in Costa Rica /Genereux et al. 2002/ showed that surface waters and shallow groundwaters were highly influenced by a mixture of high-solute bedrock groundwater from watersheds outside the study site and low-solute local water draining from hillslope soils within the studied watersheds. Deep groundwater constituted as much as 49% of the baseflow in some streams and up to 84% of the small riparian seeps and shallow groundwater near the Salto stream. The La Selva watershed is located between the steep foothills of the Cordillera Central and the Caribbean coastal plain in Costa Rica and is characterized by mountainous terrain with low-permeability deposits and bedrock mostly of volcanic origin. /Genereux et al. 2002/ point out that the obtained results are expected from the position of the studied watershed according to /Tóth 1962, 1963/.

Watersheds at the downgradient ends of regional topographic gradients are expected to receive groundwater discharge from local recharge and also from deep regional groundwater systems. These groundwater movements may happen in other areas of the world as well. Characterization of these pathways is essential for quantifying the vulnerability of surface waters to radionuclide contamination in the event of radioactive substance release to groundwater from deep geological repositories.

3.3 Measurement techniques for quantification of groundwater discharge to surface waters

Hereafter we present a summary of available methods to measure groundwater discharge to surface waters in either inland or marine environments. The main sources of this overview are the reviews of /Kalbus et al. 2006/ focusing on the estimation of groundwater discharge to inland surface waters (particularly streams) and /Burnett et al. 2006/ focusing on the estimation of groundwater discharge to the sea, i.e. SGD fluxes. They both coincide in recommending a combination of different methods for assessment of groundwater discharge to surface waters. Other sources of information are specifically cited in the text.

3.3.1 Seepage meters

Seepage meters are the only method that is able to measure direct groundwater fluxes through bed sediments. Seepage meters provide measurements of groundwater discharge at a small scale, the cross-section area of the drum (generally ~0.25 m^2), but they may provide an integrated value per unit of coastline length when located in transects. They can also provide an estimate of salinity of the discharge and measure the flux of groundwater recharge into the sediments if this occurs instead of discharge. There are different types of seepage meters. The simplest one is that of /Lee 1977/ consisting of a bottomless 208 L drum that is connected to a plastic collection bag. As the water seeps through the sediments it will displace water trapped in the drum forcing it into the plastic bag. The main disadvantages of this manual type of seepage meter are that it is labour intensive and the resulting values are integrated over the time required to make the measurements, thereby losing the possibility to monitor temporal variability within the time span.

Other types of seepage meters are the so-called automatic seepage meters which can measure groundwater discharge rates automatically and continuously. Example of these types are: the ultrasonic seepage meter /Paulsen et al. 2001/, the dye-dilution seepage meter /Sholkovitz et al. 2003/, the electromagnetic seepage meter /Rosenberry and Morin 2004/ or the heat-pulse-type /Taniguchi and Fukuo 1993, Krupa et al. 1998/, which was able to measure groundwater discharge rates into Lake Biwa every 5 min up to several days /Taniguchi and Fukuo 1996/. More recently, /Taniguchi and Iwakawa 2001/ developed a continuous-heat type of automated seepage meter. A general limitation of all seepage meter measurements is that they might be affected by possible artifacts when they are not carried out in a relatively calm environment.

While the manual type of seepage meter has been used extensively in lakes, estuaries, coastal areas and streams, the automatic ones have only been recently developed and tested in the inter-comparison experiments for SGD assessment. In streams, however, the fluxes measured with seepage meters might not be necessarily attributed to groundwater because they may include a hyporheic flow component as pointed out by /Kalbus et al. 2006/.

3.3.2 Piezometers

Multi-level piezometers nests measure hydraulic heads in sediments at different depths /Freeze and Cherry 1979/. These measurements can then be used to estimate the hydraulic gradient and ultimately the groundwater discharge (q) to the surface water body by applying Darcy´s law: $q = -Kdh/dL$, with q being the volume of groundwater discharge per unit area per unit time, i.e, [L/T], K the hydraulic conductivity [L/T] and dh/dL the hydraulic gradient [∅]. For this purpose, estimates of K are also required. These estimates may be performed at different scales by grain size analysis, permeameter tests in situ or in the laboratory, slug and bail tests or pumping tests. Depending on the scale at which K and the hydraulic gradient are estimated, Darcy's law calculations may be regional or local /Oberdorfer 2003/.

The accuracy of the discharge estimates by this method is therefore subject to accuracy in estimates of K, which are typically quite uncertain varying over several orders of magnitude within an aquifer /Burnett et al. 2006/. Piezometer measurements can also be used in conjunction to seepage meters to obtain an estimate of K from observed hydraulic gradients and groundwater discharge rates.

If piezometer measurements are done in the inland side of a coastal aquifer, they provide estimates of the terrestrially-induced freshwater SGD. In streams, for instance, point measurements of water level at the streambed can be compared with the stream water levels to assess if the stream reach is gaining or losing water to the groundwater system.

3.3.3 Geochemical tracers

Geochemical tracers can be used to track the movement of water along different pathways when they provide a detectable signal, are conservative and relatively easy to measure. For example, stable isotopes such as ^{18}O and ^{2}H are commonly used to investigate groundwater and surface water interactions in inland water systems like streams and lakes because groundwater is generally less enriched in them than streams or lakes. Other tracers for evaluation of groundwater-surface water interactions include alkalinity, and major chemical constituents such as sodium, nitrate and silica. Moreover, trace elements such as Sr, anthropogenic gases such as chlorofluorocarbons (CFCs), electrical conductivity and naturally occurring radioactive isotopes such as radon ^{222}Rn and radium ^{223}Ra, ^{224}Ra, ^{226}Ra, ^{228}Ra can be used to assess groundwater and surface water interactions in both the inland and marine environments.

In practise, however, radium isotopes have been used to less extent in inland water systems than in marine environments due to that they are in lower concentrations in freshwaters than saline waters /Kraemer 2005/. The radium isotopes are usually adsorbed onto the surface of sediments and become mobilized in case of seawater intrusion /Moore 1996, Kraemer 2005/. In coastal environments, the radium isotopes may then be transported into the coastal waters by a mixture of freshwater and re-circulated seawater discharge. Measurements of radium in the sea are carried out on transects that extend over tens of kilometers from shore, which implies that SGD estimates from these measurements are representative of average regional scales with possible contributions from several underlying aquifers in addition to the uppermost aquifer /Oberdorfer 2003/.

Radon measurements, on the contrary, are done at a local station, but depending on how well mixed the coastal zone is, the measurements may represent a spatially integrated value /Oberdorfer 2003/. Radon and radium measurements may provide then an estimate of fresh SGD, recirculated SGD or a combination of both. In inland water systems such as streams, radon measurements can be done at different stations along the stream, providing an estimation of groundwater discharge at the local or reach scales.

In addition to the naturally occurring tracers in ground and surface waters, artificial tracers such as fluorescent dyes can also be used to evaluate groundwater discharge rates to surface waters. In this case, the tracer is introduced in the groundwater system and its movement or temporal development in concentration is monitored in the surface water system.

3.3.4 Geophysical tracers

Heat can be used as a tracer to detect and measure groundwater discharge to surface waters in either inland or marine environments. Differences in temperature between the water at the bottom sediments and in the surrounding fluid may be used to identify areas of groundwater discharge at local and also regional scales. New techniques such as infrared sensors or other remote sensing methods are available. Moreover, the groundwater discharge rates can be calculated by recording temperature-depth profiles in the stream, lake or sea beds and applying some of the available solutions for heat transport in groundwater.

This approach has been used at basin scale, for instances, by /Cartwright 1970, Taniguchi 1993/, both cited in /Anderson 2005/. Furthermore, since temperature is a parameter relatively easy and quick to measure, inexpensive and robust, two methods have been developed to estimate groundwater discharge to streams at high spatial resolution on the scale of stream reaches (see e.g. /Conant 2004/ and /Schmidt et al. 2006/).

3.3.5 Water balance approaches

The water balance equation for a basin may be used to estimate the fresh terrestrially-derived SGD to the sea. The equation is: G = P–E–T–SD–dS, where G is the groundwater discharge, P is precipitation, E is evaporation, T is transpiration, SD is surface discharge and dS is change in water storage, which is usually assumed to be negligible over large periods of time such as years. The SGD rate from this balance is normally expressed in volume per time [L^3/T]. The area where groundwater discharge occurs is then needed in order to be able to compare this estimate with those expressed as flux [L/T]. In general, this method is typically imprecise because the uncertainty associated to some components of the water balance is of the same magnitude as the discharge to be estimated.

Groundwater discharge to lakes may be estimated by using a similar water budget equation for the lake. Groundwater discharge to streams, however, may be estimated by measuring the stream flow discharge in successive cross-sections and calculating the difference between them. This difference is then attributed to the exchange with groundwater. This method should be performed under low stream flow conditions to assure that any increase in the stream flow is due to groundwater and not to quickflow from a rainfall event.

In general, there are two different methods to measure stream flow discharge: velocity gauging methods or dilution gauging methods. With the first method, only the net exchange of groundwater with the stream is possible to estimate. However, with a combination of the two methods, the groundwater discharge or recharge rates can be obtained, in addition to the net exchange. This method relies on accurate measurements of stream flows and estimates of other possible inflows and outflows within the reach between the cross-sections.

3.3.6 Hydrographic analysis

This method, consisting in calculating the stream hydrograph (plot of the stream flow discharge as function of time) and separating the baseflow, is usually used to estimate the discharge of groundwater to streams. It is based on the assumption that the only contribution to baseflow is by groundwater, so the method is not valid if other possible sources of water to stream flow are present. The resulting groundwater discharge is usually an estimate on the reach scale and the accuracy of the method is constrained by the number of gauging stations.

This method has also been used to estimate SGD to the sea assuming that the discharge of groundwater to the sea in areas adjacent to streams is the same as the baseflow. By this method, only the fresh SGD fraction from the uppermost unconfined aquifers which are hydraulically connected to the stream is estimated, excluding the possible discharge from deeper confined aquifers /Oberdorfer 2003/. As for the water balance method, a limitation of the hydrographic analysis is that the uncertainties in the hydrograph terms can be of the same order of magnitude as the discharge being estimated.

3.4 Modelling techniques of groundwater discharge to surface waters

Traditionally, numerical modelling of stream-aquifer systems in inland freshwater environments has been carried out using a single model approach by which either surface water or groundwater is modelled in detail while highly simplified representations are adopted for the other component. This approach is, however, not appropriate to investigate groundwater and surface water flow interactions at regional scale /Werner et al. 2006c/.

A better approach is the use of coupled stream-aquifer interaction models. In this sense, MODFLOW /McDonald and Harbaugh 1988/, which is a traditional groundwater flow model, has been coupled with other models such as, for instance, the Streamflow Routing Package /Prudic 1989, Prudic et al. 2004, Niswonger and Prudic 2005/, MODBRANCH /Swain and Wexler 1996/, DAFLOW /Jobson and Harbaugh 1999/ or SWAT /Sophocleous and Perkins 2000/.

Recently, another MODFLOW-based coupled model, MODHMS /Hydrogeologic Inc. 2003, Panday and Huyarkon 2004/, has been developed. This model is able to simulate stream-aquifer interactions and solute transport on a regional scale. /Werner et al. 2006c/ present an application of MODHMS for simulating regional-scale surface water-groundwater interactions. More applications are needed in order to test the capabilities of this model. Other models similar to MODHMS which are able to simulate the coupled groundwater-surface water interactions and solute or heat transport processes are presented in section 4.

In a similar way as for modelling groundwater-stream interactions, the traditional MODFLOW code has also been used in combination with certain packages (LAK1, LAK2, LAK3) to simulate groundwater-lakes interactions /Hunt et al. 2003/. A competitive approach is the one based on analytical element techniques. Using such technique, /Haitjema 1995/ developed a lake package that added to the groundwater flow model GFLOW is able to simulate groundwater-lake interactions /Hunt et al. 2003/.

In near-coastal environments, simulation of total groundwater discharge to the sea (the fresh and the re-circulated fractions) requires numerical models to be able to simulate the coupled density-dependent flow and solute transport equations resulting from the interactions between the fresh groundwater and the seawater. Although several different models suitable for this purpose have been available in the past (e.g. SUTRA /Voss 1984/ or FEFLOW /Diersch 1996/), they have only recently been used to estimate SGD /Destouni and Prieto 2003, Smith and Zawadzki 2003, Smith 2004, Shibuo et al. 2006/. /Kaleris et al. 2002/ used different numerical models to simulate SGD at the Eckernförde Bay in the western part of the Baltic Sea covering an area of about 70 km^2. The resulting SGD from the 3D modelling of the groundwater flow in the studied area ranged from 1,577 $m^3/yr/m$ of coastal length to 2,208 $m^3/yr/m$ of coastal length for different modelled scenarios.

Recent modelling developments in this area comprise also the coupling of a surface water flow and transport code (SWIFT2D) with a variable-density groundwater flow and transport module (SEAWAT) to simulate the coupled surface water and groundwater flow and salinity system in coastal wetlands and estuaries /Langevin et al. 2005/. Further relevant modelling development for the study of groundwater-surface water interactions is reported in section 4.

4 Modelling tools for hydrosystem analysis

Hydrosystem analysis refers to the analysis of the integrated soil, surface and groundwater systems in a catchment including their interactions with the atmosphere and biosphere. Some conceptual models and numerical codes for hydrosystem flow analysis and solute mass or heat transport are: MIKE SHE developed by the Danish Hydrologic Institute (DHI), the HEC-HMS (Hydrologic Model System) developed by the USA Army Corps of Engineers, the HSPF (Hydrological Simulation Program-Fortran) jointly developed by the USGS and US EPA, the InHM (Integrated Hydrology Model) developed by the University of Waterloo and Stanford, MODHMS /Hydrogeologic Inc. 2003, Panday and Huyarkon 2004/, HydroGeoSphere /Therrien et al. 2006/ and GeoSys/RockFlow /Kolditz et al. 2006a/. This section describes briefly the main characteristics of two of these tools, the HydroGeoSphere and the GeoSys/RockFlow codes, which although still under development by the Universities of Waterloo and Tübingen, respectively, are considered very promising for hydrosystem analysis.

4.1 HydroGeoSphere

HydroGeoSphere /Therrien et al. 2006/ is a fully-coupled surface and subsurface flow and transport code jointly developed by the Groundwater Simulations Group and Hydrogeologic, Inc. The subsurface water module is based on the three-dimensional subsurface flow and transport code FRAC3DVS jointly developed at the University of Waterloo and Université Laval. The surface module is based on the Surface Water Flow Package of the MODHMS code developed by Hydrogeologic, Inc.

While FRAC3DVS uses a 3D numerical approach to simulate steady-state/transient, variably saturated flow and advective-dispersive solute transport in porous or discretely fractured porous media, MODHMS was created by modifying the MODFLOW code to simulate 3D variably saturated subsurface flow, 2D areal overland flow, and flow through a network of 1D channels, including natural streams and man-made canals, pipes, or tile drains. HydroGeoSphere has been developed by incorporating a modified version of MODHMS into the FRAC3DVS code.

HydroGeoSphere is a powerful tool with a unique feature which is the possible simultaneous resolution of the surface and variable saturated flow regimes as well as the solute concentrations in both flow domains at each time step. By this full-integrated simulation mode the flow of water is allowed to partition from precipitation into different possible water domains, such as overland and stream flow, evaporation, infiltration, recharge and subsurface discharge into surface waters, and in addition, the dissolved solutes are permitted to be exchanged between the surface and the subsurface water systems.

The complete hydrologic cycle is modelled using physically based equations of all components in one integrated code. While the subsurface system can be represented as 3D, the surface system can be represented as 2D areal flow for the entire surface or 2D runoff into 1D channels. The code is able to model the transport through the different water systems for both non-reactive and reactive chemical species. It can handle fluid and mass exchange between fractures and matrix including matrix diffusion effects and solute advection in the matrix and also chain-reactions of radionuclide substances. The code is written in FORTRAN 95. It is robust and supported by a user-friendly interface, which may be used to prepare input data or visualize the results using, for instance, 3D animations. An illustrative example of the use of this code is presented by /Randall 2005/ for the analysis of seasonally varying flow in the crystalline rock watershed of Bass Lake in Canada. More recent applications of this code are reported by /Rivett et al. 2006/ and /Savard et al. 2007/.

One general difference between HydroGeoSphere and MIKE SHE, which is the code selected by SKB for near surface hydrological and hydrogeological investigations /SKB 2006/, is the fact that the MIKE SHE code is modular /Graham and Butts 2005/ where each model runs independently of one another and mutually exchanges water on each time step. The HydroGeoSphere code, on the other hand, can use both an integrated finite difference or an integrated finite element approach to solve the flow of water and solutes in the different components of a watershed simultaneously for each time step /Therrien et al. 2006/. Additionally, MIKE SHE is flexible in the sense that allows the user to choose between lumped and conceptually based approaches or distributed and physically based equations for each hydrological process /Graham and Butts 2005/, while HydroGeoSphere is exclusively a physically-based code /Therrien et al. 2006/.

With regard to the discretization method used, HydroGeoSphere allows several discretization options ranging from simple rectangular and axisymmetric domains to irregular domains with complex geometry and layering /Therrien et al. 2006/, while MIKE SHE allows only square grid cells in the surface domain, i.e. in the x- and y- directions /Randall 2005/. Finally, while HydroGeoSphere may be used to simulate subsurface groundwater flow in an arbitrary combination of porous, discretely-fractured and dual porosity media /Therrien et al. 2006/, MIKE SHE can simulate flow in porous media and/or media with dual porosity /DHI 2007/.

4.2 GeoSys/RockFlow

GeoSys/RockFlow /Kolditz et al. 2006a/ is an object-oriented, finite element simulator applicable to a wide range of thermo, hydro, mechanical and chemical problems in geosciences. It started to be developed at the University of Hannover in 1985 and is currently being continuously developed jointly at the University of Hannover and at the University of Tübingen.

The code, written in C/C++, is able to simulate hydromechanical processes such as groundwater flow in confined and unconfined aquifers, multi phase flow and gas flow, fracture flow, dual continua, density dependent flow due to thermal or salinity effects, river flow and overland flow. Coupled to the flow field, it is also able to simulate heat transport with density and viscosity changes and non isothermal multiphase flow with phase changes as well as transport of different chemical species with density changes, equilibrium and kinetic chemical and biogeochemical reactions and sorption /Kolditz et al. 2006b/.

In the field of geomechanics, the code is able to simulate mechanical processes such as poro-elasticity, thermo-elasticity, visco-elasticity (creep), elasto-plasticity (hardening) and dynamic deformation. Some recent developments and applications of the code are presented, for instance, by /Beinhorn 2005/ and /De Jonge 2005/. /Beinhorn 2005/ focuses on implementing the surface and subsurface water flow systems and solute transport into the GeoSys/RockFlow code. /De Jonge 2005/ focuses, however, on developing the GeoSys/RockFlow code to allow simulation of thermal and hydraulic processes and their combined effects in low-permeable porous media such as bentonite. He also applies the code to different problems in order to validate it. For instance, he illustrates that the code successfully simulates the desaturation process of bentonite due to heating in a closed system.

5 Application Forsmark

In this section, we use the developed (in section 2.2) general conceptual framework for performing an initial demonstration analysis of solute transport through coupled ground-surface-coastal water systems of Forsmark. We consider different transport scenarios, in order to clarify and explain research questions that may be of critical importance for the relation between, on the one hand, (deep) subsurface source distributions and extents, and on the other hand, resulting solute distributions in the shallow water system. We also summarize the flow model and data processing that underpin the transport results (described in detail in /Jarsjö et al. 2004, 2006/), noting however that the conceptual framework is model-independent and may hence be equally appropriate in other hydrological model contexts.

5.1 Site model and GIS data processing

Figure 5-1 shows close-ups of the here considered 29.5 km^2 Forsmark model area, containing 10 focused outlets (numbered blue squares in Figure 5-1) and their catchments (coloured areas in Figure 5-1). The model area extends all the way to the coast, including very small coastal catchments (grey in Figure 5-1), limited by the grid resolution of 10×10 m. Quaternary deposits cover a major part of the surface and are dominated by till (mainly sandy). Furthermore, the groundwater levels are shallow (e.g. with a mean annual level of 1 metre below the surface in monitoring wells of Forsmark), and land is mainly covered by forest. Lakes and wetlands are relatively common, with the wetlands, which can be partially forested, covering up to 20% of the area. Water courses are generally small. For further details, see e.g. /Lindborg 2005/. The total number of considered coastal outlets (also limited by the grid resolution) is 1,532. Before performing the hydrological modelling and analyses (described in the sections 5.2 to 5.6), the (input) GIS data was pre-processed as summarised in this section.

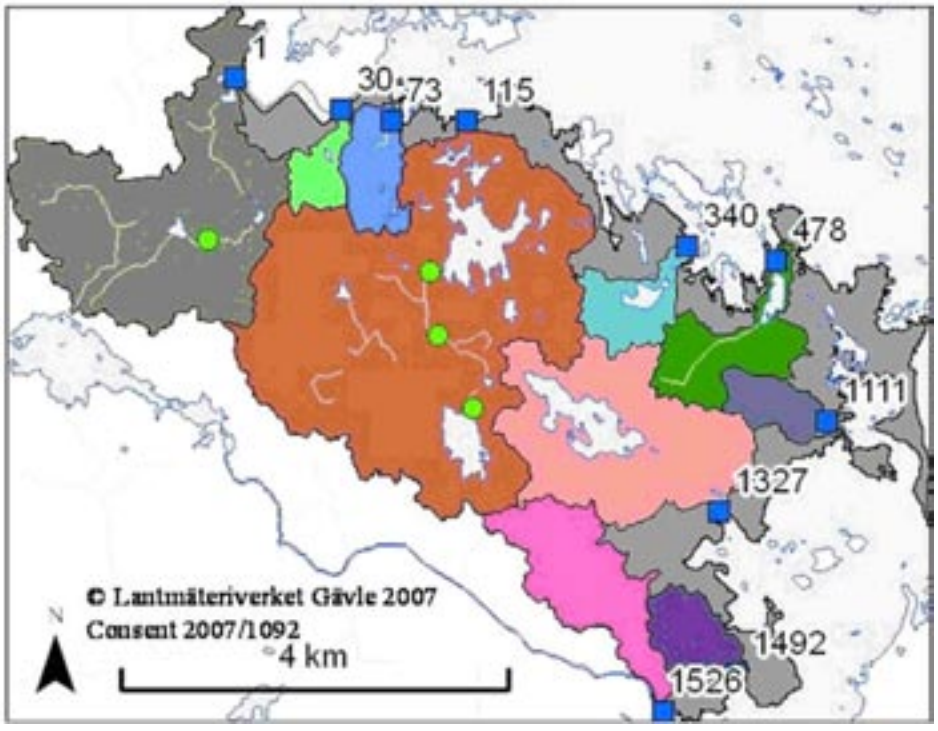

Figure 5-1. *Main catchments (coloured), small coastal catchments (grey), main catchment outlets (numbered, filled blue squares) and measurement stations (filled green circles) of the Forsmark area.*

The original digital elevation models (DEMs) for Forsmark and Laxemar-Simpevarp are based on ortophoto maps and have a resolution of 10×10 m. /Brydsten 2004/ and /Brydsten and Strömgren 2004/ gave special attention to the representation of the current shoreline at elevation 0. A combination of field measurement DGPS data on shoreline location and manually digitised shoreline location with IR orthophoto was used to increase the accuracy of this 0-isoline. We further processed the DEM by use of the standard pit-filling function in the ArcGIS Hydrology modelling tool extension and by lowering the DEM by 3 m at field-controlled stream locations (including man-made ditches) and lakes. The processing aimed at increasing the accuracy of the subsequent flow direction determination (following the principles described further in section 5.2), which was also performed using the ArcGIS Hydrology extension. As a result, the derived catchment delineations shown in Figure 5-1, obtained using a PCRaster toolbox /Van Deursen 1995/ on the basis of the modified DEM, were consistent with independently field-controlled boundaries of the larger catchments within the model areas /Brunberg et al. 2004/.

The annual mean precipitation over the model area was determined by using 30-year average values from the standard normal period (1961–1990) from nearby measurement stations operated by the Swedish Meteorological and Hydrological Institute (SMHI), reported in /Larsson-McCann et al. 2002/. Specifically, we derived average precipitation maps and average temperature maps through spatial interpolation of measurement data from four SMHI stations in the Forsmark model area vicinity /Jarsjö et al. 2004, 2006/. The temperature data was used in combination with precipitation data as input in the determination of actual evapotranspiration (E_a), according to one of the two considered evapotranspiration modelling methods further described in section 5.2.1 (E_a-method (i), Equation 5.4a).

Soil data for most part (around 70%) of the Forsmark area were obtained from detailed digital maps of /Sohlenius et al. 2004/. The maps can be presented in scale 1:10,000 and show the spatial distribution of Quaternary deposits and bedrock outcrops, including all features larger than 10×10 m. The detailed Forsmark map was complemented with mapping of the Geological Survey of Sweden at a 1:50,000 scale. The vegetation data were obtained from mapping of /Boresjö Bronge and Wester 2002, 2003/, showing the distribution of different kinds of forest, open land and wetland. Rock outcrops are recorded to different classes, such as forest classes or open land classes, according to prevailing vegetation. Data sources used by /Boresjö Bronge and Wester 2002, 2003/ include geo-referenced SPOT4 XI data (20 m ground resolution), geo-referenced Landsat TM data (30 m ground resolution), soil type data, topographic map data and colour infrared aerial photographs.

The soil and vegetation data was used in combination with precipitation data as input in the determination of E_a according to the second considered evapotranspiration modelling method described in section 5.2.1 (E_a-method (ii), Equation 5.4b). Because this E_a-method (ii) quantifies local evapotranspiration variability based on a 6×2 soil texture/land-cover matrix (plus an additional water/wetland class), the numerous original soil and vegetation data classes were re-classified and condensed (see /Jarsjö et al. 2006/).

5.2 Flow quantification

5.2.1 Methodology

The PCRaster modelling approach requires a discretisation of the model domain into quadratic cells of equal size. The full model domain in Forsmark covers 10×6 km, and the domain was discretised into 600,000 cells (including also inactive cells outside of the considered catchments of Figure 5-1) of size 10×10 m. As input for the hydrological modelling module in PCRaster, each grid cell was assigned properties of ground slope, slope direction, precipitation, temperature, land cover, vegetation, aquifer porosity and aquifer capacity. Some of these basic properties, or input data, were pre-processed before running the hydrological modelling module (see further section 5.1). We used ESRI-Arc GIS 8.2 to handle the properties of the catchment in this pre-processing.

Using calculation schemes of the hydrological modelling module in PCRaster and in consistency with the POLFLOW model of /De Wit 1999, 2001/, a precipitation surplus PS is calculated for each grid-cell (in mm/year) as the difference between the precipitation, P, and actual evapotranspiration, E_a:

$$PS = P - E_a \qquad \text{Equation 5.1}$$

Two different and independent methods are used in this study to estimate the E_a-term in Equation 5.1, in accordance with e.g. /Darracq et al. 2005/. The resulting total runoff of water precipitated within the cell, R (mm/year), must be equal to PS (Equation 5.1) at steady-state and may be further divided into a surface runoff and soil interflow contribution R_S, and a groundwater discharge contribution R_{gw}

$$R = R_S + R_{gw} = PS \qquad \text{Equation 5.2}$$

The groundwater discharge R_{gw} may locally be expressed as a certain fraction f ($0 \le f \le 1$) of R implying that R_S then can be expressed as $(1-f)\cdot R$, such that Equation 5.2 is fulfilled. We here focus on total coastal discharges and need therefore not make use of any specific relations regarding the distribution of total flows into groundwater and surface water flows within the catchment. Instead, for the resulting coastal discharges, we use field-controlled land-use, vegetation and stream network information for distinguishing between surface water flows and groundwater flows.

For estimation of the total water discharge Q [L^3/T] through each grid cell, local flow directions are estimated on the basis of the digital elevation model. Each cell is then associated with a unique flow direction, into the neighbouring cell with the lowest elevation. Furthermore, a sub-catchment area Ω_i is defined for each cell i, including all upstream cells that contribute to Q_i through cell i, on the basis of all upstream defined flow directions. Using this definition of Ω_i, the average water discharge Q_i [L^3/T] through an arbitrary cell i during the considered simulation period (here primarily annual averages) is given by:

$$Q_i = \left(PS_i + \sum_{\Omega_i} PS \right) \cdot A_{cell} \qquad \text{Equation 5.3}$$

where A_{cell} is the cell area (all cells must have the same A_{cell} in PCRaster).

The flow Q represents the total discharge from each cell to downstream areas. An underlying assumption is then that the sub-catchment areas and mean groundwater flow directions are essentially similar to those of surface water. Although PCRaster in principle allows for other assumptions, we note that the available independent water balance data from modelled sub-catchments at least do not indicate the existence of surface or subsurface water catchment boundaries that are considerably different from the ones used here.

/Jarsjö et al. 2004, 2006/ modelled runoff in the Forsmark area by use of two independent methods for calculation of average annual evapotranspiration E_a. In the first method, the mean actual evapotranspiration is quantified on the basis of annual mean temperature and precipitation. In the second method, local evapotranspiration is related to soil and land cover (lc) characteristics (empirically determined based on conditions in German catchments).

Evapotranspiration methods (i) and (ii) use the following principal parametric formulations for the actual evapotranspiration matrix $\mathbf{E_a}$ and corresponding (site-specific) spatially averaged evapotranspiration values:

$$\mathbf{E_a^{(i)}} = X_{cal} \cdot \mathbf{E_a^{Turc}}(\mathbf{T},\mathbf{P}); \qquad \overline{E}_a^{(i)} = X_{cal} \cdot \frac{1}{A_\Omega} \int_\Omega \mathbf{E_a^{Turc}}(\mathbf{T},\mathbf{P})\mathrm{dA} \qquad \text{Equation 5.4a}$$

$$\mathbf{E}_{\mathbf{a}}^{(\mathbf{ii})} = X_{cal} \cdot \mathbf{E}_{\mathbf{a}}^{\mathbf{Wend}}(\mathbf{soil},\mathbf{lc}); \qquad \overline{E}_{a}^{(ii)} = X_{cal} \cdot \frac{1}{A_{\Omega}} \int_{\Omega} \mathbf{E}_{\mathbf{a}}^{\mathbf{Wend}}(\mathbf{soil},\mathbf{lc})\mathrm{dA} \qquad \text{Equation 5.4b}$$

where **T**, **P**, **soil** and **lc** are the temperature, precipitation, soil and land cover matrices, Ω is the spatial extent of the considered catchment(s), A_Ω is the area of Ω, $\mathbf{E}_{\mathbf{a}}^{\mathbf{Turc}}$ and $\mathbf{E}_{\mathbf{a}}^{\mathbf{Wend}}$ are the empirical E_a relations of /Turc 1954/ and /Wendland 1992/, respectively, see also /Jarsjö et al. 2004/, and X_{cal} is a scaling factor allowing calibration of the regional average evapotranspiration considering independent estimates of specific (area-averaged) runoff, as further explained in /Jarsjö et al. 2006/ and /Jarsjö et al. 2008/.

5.2.2 Coastal discharges

The focused discharges through point outlets, appear to the right of the solid, vertical line in Figure 5-2. These discharges are shown by black bars in Figure 5-3 and contribute to 80% of the total discharge in Forsmark. The fact that all the crosses representing point outlets coincide with the diagonal 1:1-relation (illustrated by the grey line in Figure 5-2) shows that E_a-method (i) and (ii) (see section 5.2.1) yield practically identical relative discharges, which means that these relative discharges and the flow variations between outlet points are robust with respect to investigated uncertainties in local evapotranspiration values. However, Figure 5-2 shows that the deviations from the 1:1-relation of Figure 5-2 are considerably larger for the diffuse small coastal discharges, indicating that local predictions of specific point values within a diffuse coastal discharge field are more uncertain. Specifically, it is the larger spread of the crosses in the lower, left region of the graph that shows that smaller local discharge values within a diffuse discharge field are associated with greater prediction uncertainties.

Figure 5-3 shows the modelled absolute coastal discharges from the Forsmark catchment into the Baltic Sea, combining here for simplicity the results of the two considered E_a-methods by averaging their output (the differences were presented separately in Figure 5-2). Figure 5-3 specifically shows pixel-by-pixel total coastal discharges, with each 10×10 m coastal pixel being represented by a bar. The x-axis shows distances measured along the coastline (excluding islands, see the line between the grey catchment areas and the water of Figure 5-1), starting in NW. Black bars in Figure 5-3 mark focused surface water discharges. Each marked surface water discharge bar contributes individually to 1% or more of the total coastal discharge and

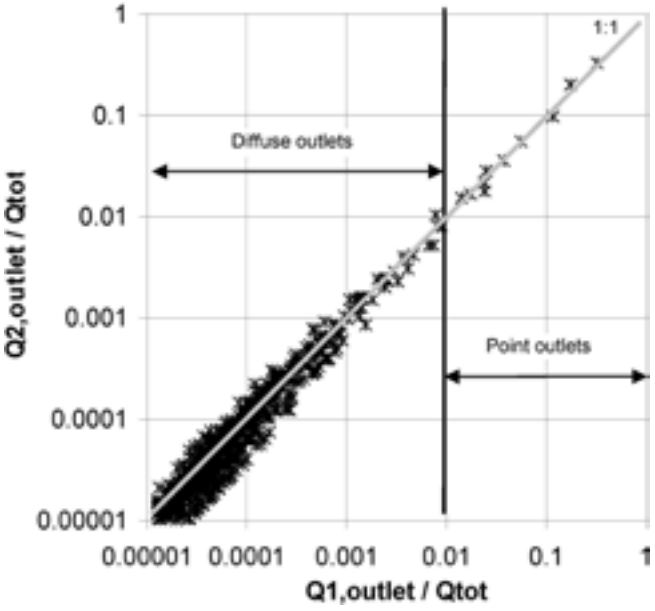

Figure 5-2. *Distribution of total flow among coastal outlets (comparison between E_a-prediction methods (i) and (ii).*

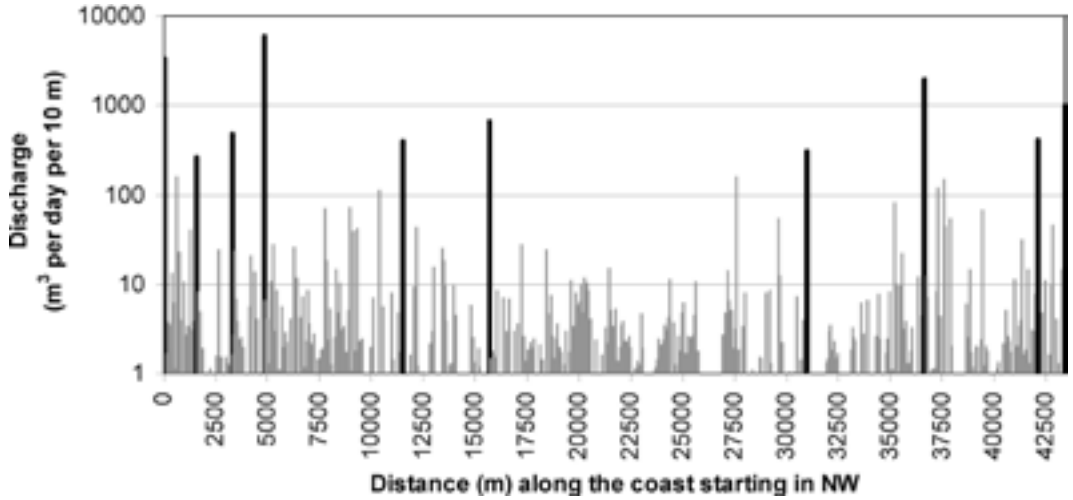

Figure 5-3. *Estimated coastal discharges from the Forsmark catchment into the Baltic Sea.*

constitutes a visible stream. At the remaining locations (grey bars), the diffuse coastal discharge occurs through groundwater flow, although at some of these locations, surface water may temporarily form when conditions are wet.

Altogether, there are 10 focused surface water outlets in Forsmark. The locations of these outlets are shown by the numbered, filled blue squares in Figure 5-1 (with blue square number 1 in Figure 5-1 corresponding to the leftmost black bar in Figure 5-3, and blue square number 1526 in Figure 5-1 corresponding to the rightmost black bar in Figure 5-3). The catchment areas of these focused outlets are in Figure 5-1 shown in various colours. Furthermore, the grey region located in the relative vicinity of the coastline in Figure 5-1 indicates the catchment areas for the diffuse groundwater flows (grey bars in Figure 5-3). Regarding the ratio between the focused surface water discharges along the coast and the total coastal discharge (surface water + groundwater) results show that 80% of the discharge is focused (and hence the remaining 20% is diffuse, see also /Jarsjö et al. 2006, 2008/. This result corresponds also well to the monitored (coloured) / unmonitored (grey) area-ratios of corresponding catchment areas shown in Figure 5-1.

5.3 Mean advective travel time

The PCRaster maps of precipitation, calibrated evapotranspiration, runoff, vegetation, soil texture, slope, and flow directions, which were produced by /Jarsjö et al. 2004, 2006/ and resulted in the discharges shown in the above section 5.2, are here used as model input. The grid cell resolution of the model is 10×10 m.

The mean groundwater flow velocity is calculated for each cell in the PCRaster model as $v = K \cdot (gradient)/n$, where K is the mean hydraulic conductivity, *gradient* is the hydraulic gradient, and n is the mean effective porosity. The mean hydraulic conductivity is assumed to be $1.5 \cdot 10^{-5}$ m/s, which equals the mean value in the Quaternary deposits-bedrock interface estimated by /Johansson et al. 2005/. The numerous slug tests that have been performed in the area have indicated that the hydraulic conductivity on average is larger in the Quaternary deposits-bedrock interface than higher up in the Quaternary deposits /Johansson et al. 2005/. The effective porosity is assumed to be 0.05, which also equals the mean value in the Quaternary deposits-bedrock interface estimated by /Johansson et al. 2005/.

We focus on transport pathways originating from deep groundwater, within which flow may be relatively unaffected by small-scale variations in surface elevation. We therefore assumed that within each one of the catchments of the 1,532 coastal outlet cells, the hydraulic gradient equals the mean ground slope of all 10×10 m PCRaster cells in the corresponding area, so that the

hydraulic gradient is constant along each streamline and positive even where the mean ground slope is zero (e.g below lakes). This is the basic assumption used for all three transport scenarios of section 5.3.1. In the uncertainty analysis of section 5.6.1, we then consider how an alternative assumption, i.e. that flow along the considered pathways is governed by hydraulic gradients that equal the local (10×10 m grid) ground slope, affects the results. The mean ground slope in each PCRaster cell was derived from the elevation map by /Jarsjö et al. 2004/. Unfortunately, the digital elevation map, and, consequently, the resulting slope map and flow direction map, did not include Lake 7:1 in the north-eastern part of the model area. As a result, the mean groundwater flow velocity could not be calculated for the cells within Lake 7:1.

The two hydrological factors in Equations 2.4b and 2.4c, β_{gw} and γ_{gw-s}, may vary spatially over the model area. Streams, lakes and wetlands that have surface water connection with the coast may normally be characterised by $\beta_{gw} = 0$. These surface water networks where no groundwater recharge is assumed to take place will from now on be referred to as *surface water systems*. The factor γ_{gw-s} may take on any value between 0 and 1. In regions characterized by $\gamma_{gw-s} = 0$, all released pollutants/nutrients will be discharged to the recipient by groundwater, whereas all flow paths from regions where $\gamma_{gw-s} = 1$ will go through a surface water system on their way down to the recipient.

In Figure 5-4, all lakes, streams and wetlands in the Forsmark model area can be seen. The names of six of the main lakes are given. The reader is referred to /Johansson et al. 2005/ for the names of other lakes and locations of measurement point. The lakes, streams and wetlands that are parts of surface water systems are shown in Figure 5-5. Within the surface water systems, which represent 15% of the model area, it is assumed that none of the precipitation surplus will yield groundwater, i.e. $\beta_{gw} = 0$. In the rest of the model area, the entire precipitation surplus is assumed to pass through the groundwater system on its way out to the sea, in other words, β_{gw} is assumed to be 1.

The residence time of a lake or wetland is defined as $T_{Res} = A \cdot d_{eff}/Q$, where A is the area of the lake or wetland, d_{eff} is the mean effective depth, and Q is the mean inflow rate. The mean effective depth in the wetlands is defined as the product of the depth and the water content (typically around 0.9). In the lakes, d_{eff} is simply the mean depth.

/Brunberg et al. 2004/ made bathymetric maps and depth grid maps for the 25 main lakes in the Forsmark model area based on depth soundings. The lakes in /Brunberg et al. 2004/ also include some areas around the lakes that are defined as wetlands in the land cover data used in

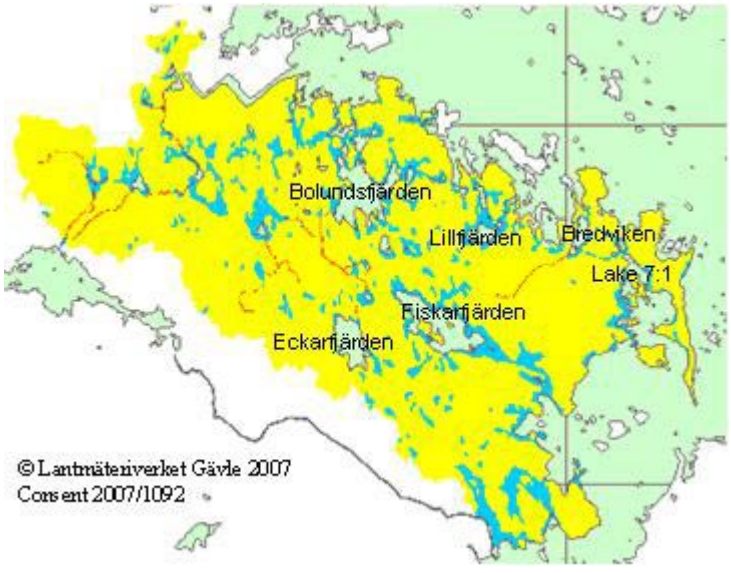

Figure 5-4. *Surface water in the Forsmark model area, with the red area representing streams, the light green area representing lakes and sea, and the light blue area representing wetlands.*

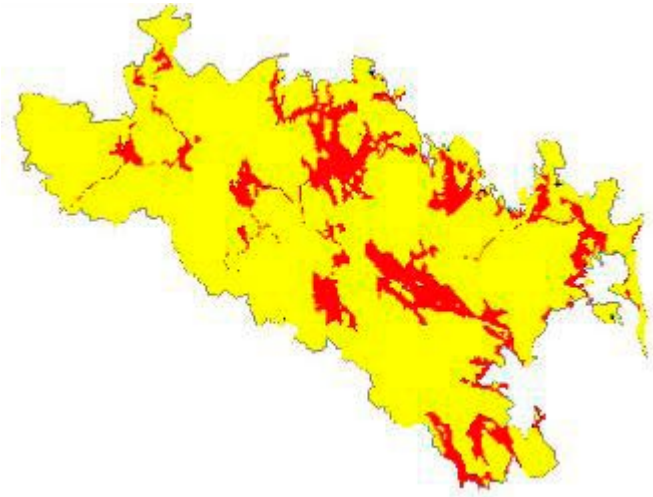

Figure 5-5. *Surface water systems connected with the coast, where β_{gw} = 0, are represented by the red area, and the rest of the model area, where β_{gw} = 1, is represented by the yellow area.*

the PCRaster modelling (see Appendix 1). Thus, the bathymetric maps and depth grid maps in /Brunberg et al. 2004/ could be used together with the mean depths given by /Brunberg et al. 2004/ to estimate the mean depth in both the lakes and the wetlands around the lakes. The mean depth of the shallowest lake, *Graven*, was estimated to 0.16 m. The estimated mean depth of the deepest lake, *Eckarfjärden*, was 1.1 m. The estimated mean depths of the wetlands around the lakes ranged between 0.1 and 0.2 m. The mean depth of the small lakes which were not morphometrically characterised in /Brunberg et al. 2004/ is generally assumed to be 0.3 m. Only if there is a larger lake nearby with a lower mean depth than 0.3 m, the mean depth is assumed to be the same as in that lake.

/Fredriksson 2004/ investigated two peatlands in the Forsmark area. He measured the depth at several locations, and estimated the mean depth to 1 m in both wetlands. The water content in the samples was approximately 90%, which is a normal value for peat. Based on these field data, the effective mean depth of the wetlands that mainly consist of peat is assumed to be 0.9 m, with the exception of the wetland south of Eckarfjärden where the measured peat layer in borehole SFM0017 was 1.1 m /Johansson 2003/ and the effective depth is assumed to be 1.1·0.9 = 1 m. In /Johansson, 2003/, the depth of one wetland without peat was also measured, namely the wetland west of Lillfjärden where the depth to the clayey till in borehole SFM0009 was found to be 0.4 m. The effective depth in that wetland is therefore assumed to be 0.4·0.9 = 0.36 m. In all other wetlands, where there is no peat according to the soil data, the mean depth is assumed to be 0.15 m, which was the most common estimated depth in the wetlands around the lakes.

The mean inflow rate Q into each lake and wetland was defined as the precipitation surplus within the lake/wetland plus the precipitation surplus of all upstream cells. The maps produced by /Jarsjö et al. 2004, 2006/ with calibrated values of flow rate and precipitation surplus in each cell were used.

The travel time in streams is defined as the stream length divided by the mean flow velocity. The mean flow velocity is defined as $v = Q/A$, where Q is the mean annual flow rate and A is the mean cross-section area of the stream. For 5 of the streams in the model area, measured cross-section areas /Nilsson and Borgiel 2004/ ranging between 0.29 and 0.43 m^2 are used. For those streams, Q is assumed to be equal to the modelled mean flow rate value /Jarsjö et al. 2004, 2006/ in the cell where the cross-section area was measured. For the remaining 7 streams where no measured values are available, the cross-section area is assumed to be 0.3 m^2. For the calculation of the mean flow velocity in those streams, we use the modelled mean Q value /Jarsjö et al. 2004, 2006/ in the mouth of the stream.

The difference between the modelled flow rate in PCRaster and the flow rate measured manually by /Nilsson and Borgiel 2004/ is quite small, and the mean travel time in all streams will be less than 1 day regardless of whether it is calculated from measured or modelled flow rates. However, all streams were found to be dry part of the year, and the travel time to the coast for particles that reach a temporarily dry stream may, of course, be much longer than 1 day. This is particularly true for the stream that flows out in Bredviken. In the measurement point PFM000073, just before the outlet to Bredviken, the stream was dry at 8 of 19 occasions, and only at one occasion the flow was high enough to be measured.

5.3.1 Considered transport scenarios

For a solute which is released in the deep groundwater and reaches the Quaternary deposits somewhere in the Forsmark model area, three scenarios for the transport pathways to the coast are considered, namely:

Scenario I – transport in the Quaternary deposits/bedrock interface only.

Scenario II – transport in the coupled groundwater-surface water system.

Scenario III – half of the solute is transported as in scenario I, half as in scenario II.

In scenario I, $\gamma_{gw\text{–}s} = 0$ in all cells, which means that the solute is transported in the Quaternary deposits-bedrock interface under streams, lakes and wetlands all the way out to the outlet to the Baltic Sea. In scenario II, the solute is only transported in the groundwater if there is no surface water above. As soon as it reaches a cell defined as stream, lake or wetland in the land cover map, it leaves the groundwater and is transported along the flow direction in the surface water instead. A flow path may go through isolated lakes and wetlands and then through groundwater again until reaching a surface water system that leads out to the sea. Hence, a conservative solute which reaches the Quaternary deposits under a surface water system (where $\beta_{gw} = 0$) or in cells upstream of surface water systems (where $\gamma_{gw\text{–}s} = 1$) will always be transported out into the sea by surface water.

The remaining small coastal sub-catchments with no surface water outflow into the sea (where $\gamma_{gw\text{–}s} = 0$) represents 11% of the total model area (see Figure 5-6). In scenario III, $\gamma_{gw\text{–}s} = 0.5$ in all cells upstream of or within surface water systems, which means that 50% of the flow paths from this area will go in the Quaternary deposits-bedrock interface all the way out to the sea, in accordance with scenario I, whereas 50% of the flow paths will leave the groundwater as soon as they reach surface water, in accordance with scenario II.

5.3.2 Calculation of advective travel times for the different scenarios

The PCRaster function *ldddist* is used to calculate the physical travel time from each cell in the model area to a coastal outlet assuming scenario I, or to either a coastal outlet or a surface water system connected with the sea assuming scenario II–III. The mean travel time is calculated in such a way that the flow length from a cell to the first downstream cell is divided by the mean flow velocity in the two cells. The program then adds all these cell-to-cell travel times until that cell that is defined as the end of the flow path. In Figure 5-7, the mean travel times from each one of the cells out to the coast are shown for scenario I and scenario II. In Figure 5-7a, corresponding to scenario I, the flow paths are assumed to go in the Quaternary deposits-bedrock interface all the way out to the sea. In Figure 5-7b, corresponding to scenario II, the flow paths only go in the subsurface in the cells where there is no stream, lake or wetland. In scenario III, the travel time along half of the flow paths in each cell is equivalent to the travel time in scenario I, whereas the travel time along the other half corresponds to the travel time in scenario II. As already has been mentioned, no groundwater flow velocity could be calculated and no flow directions could be generated for the cells within Lake 7:1. In the case of transport in groundwater only from cells upstream of Lake 7:1, the travel time to the outlet into Lake 7:1 has therefore been calculated instead of the travel time to the coastal outlet.

Figure 5-6. *The small coastal sub-catchments with no surface water outflow into the sea (where* $\gamma_{gw-s} = 0$ *for all considered transport scenarios) are represented by the red area. Areas defined as surface water systems and the area upstream of those surface water systems are represented by the yellow area.*

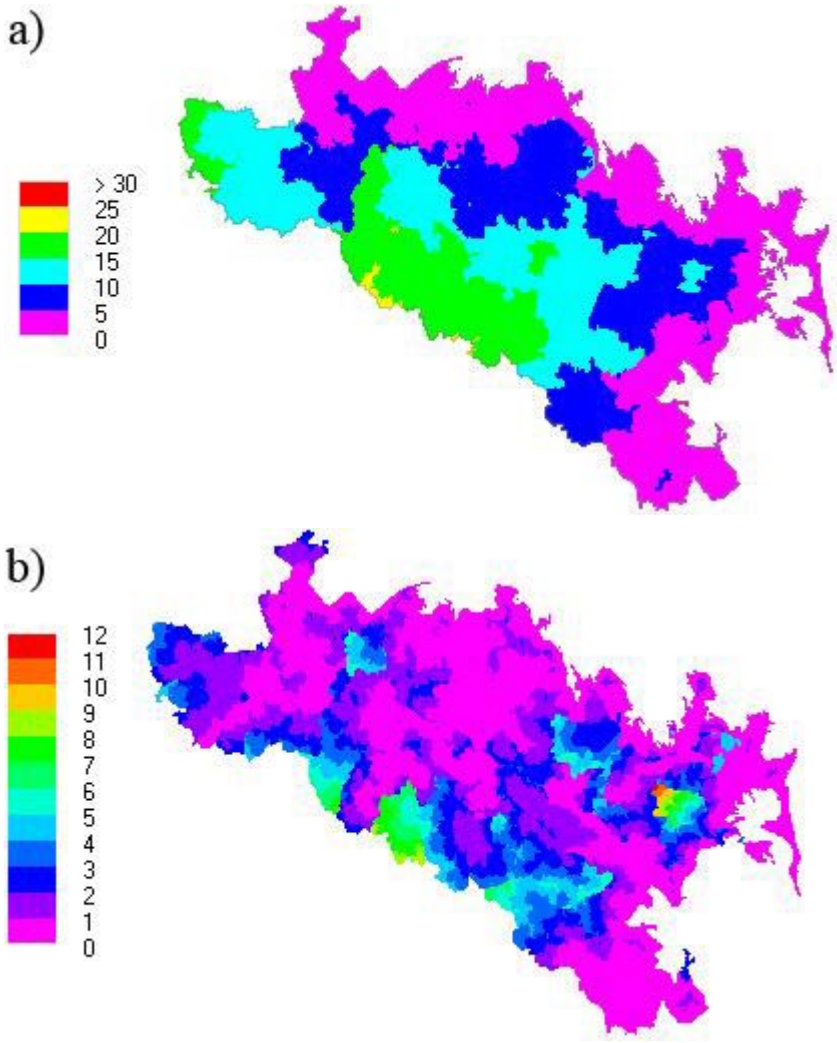

Figure 5-7. *Mean advective travel time (years) to the coast for (a) scenario I, where the transport takes place in groundwater only, and (b) scenario II, where the transport takes place in groundwater, streams, lakes and wetlands.*

For isolated lakes and wetlands that do not have any surface water connection with the sea, an effective flow velocity $v = L_{eff}/T_{Res}$ is assumed in scenario II and for half of the flow paths in scenario III. L_{eff} is an effective flow length and T_{Res} is the residence time. The effective flow length is defined as the diameter of a circle with the same area A as the lake or wetland, i.e. $L_{eff} = \text{sqrt}(4 \cdot A/\pi)$. When the solute reaches a surface water system which is connected with the sea, the remaining travel time to the coast is assumed to be the sum of the residence times of all downstream lakes, wetlands and streams.

5.4 Mean advective travel times for the different scenarios

Figures 5-8 to 5-13 show mean advective travel time distributions for the entire model area and for different subareas. The mean advective travel time distribution for an area A is equivalent to the frequency of occurrence of different mean advective travel times within A. As describe above, the mean advective travel time from each cell in the model area out to the coast is calculated for scenario I–II, whereas two different mean travel times correspond to each cell in scenario III, one for the flow paths that will only go in the Quaternary deposits-bedrock interface and one for the flow paths that may pass the surface water system before they reach the coast and the sea.

For scenario II–III, the travel time for the shorter pathways that end in the (terrestrial) surface water system is also calculated. The frequency of a travel time t within an area A is calculated in such a way that the area of the subarea within A from where the travel time $T \approx t$ is divided by the total area of A. The frequency of different travel times then gives the travel time distribution. Figure 5-8 illustrates the distribution of mean advective travel times to a surface water system. In scenario II, this is the distribution of the travel time to a surface water system from all upstream cells, whereas it in scenario III corresponds to the travel time distribution of the fraction of flow paths that actually reach a surface water system. Figure 5-9 shows the distribution of mean advective travel times from the area upstream of the surface water system (i.e. the same area as considered in Figure 5-8) through groundwater and surface water all the way out to the coast.

The travel time distributions in Figure 5-8 and Figure 5-9 are almost identical since the travel times through the surface water systems out to the sea is relatively short, as can be seen in Figure 5-10, where the distribution of the mean advective travel times from the cells within the surface water systems out to the coast is shown. Figure 5-11 illustrates the distribution of mean advective travel times to the coast from cells within coastal sub-catchments without surface water outflow (e.i. where $\gamma_{gw-s} = 0$ in all scenarios). Figure 5-12 and Figure 5-13 show the distribution of mean advective travel times from all cells in the model area out to the coast for scenario I and scenario III respectively.

5.5 Delivery factors considering different attenuation rates

Once the mean advective travel time to the recipient is estimated for a given cell in the model area, a delivery factor α can be calculated for that cell by use of the Equations 2.5c–d. The delivery factor then represents the fraction of the solute released in the cell that is expected to reach the recipient. The Figures 5-14 and 5-15 show the delivery factors to the coast for all cells in the model area considering different first order attenuation rates λ [year^{-1}] for scenario I and scenario II. The delivery factors in scenario III are equal to the mean of the delivery factors in the other two scenarios. To minimise the risk to underestimate delivery factors, retardation due to sorption of the solute is not considered. If attenuation takes place both in the aqueous and the sorptive phase, which is the case for radioactive decay, sorption would reduce the amount of the solute reaching the recipient.

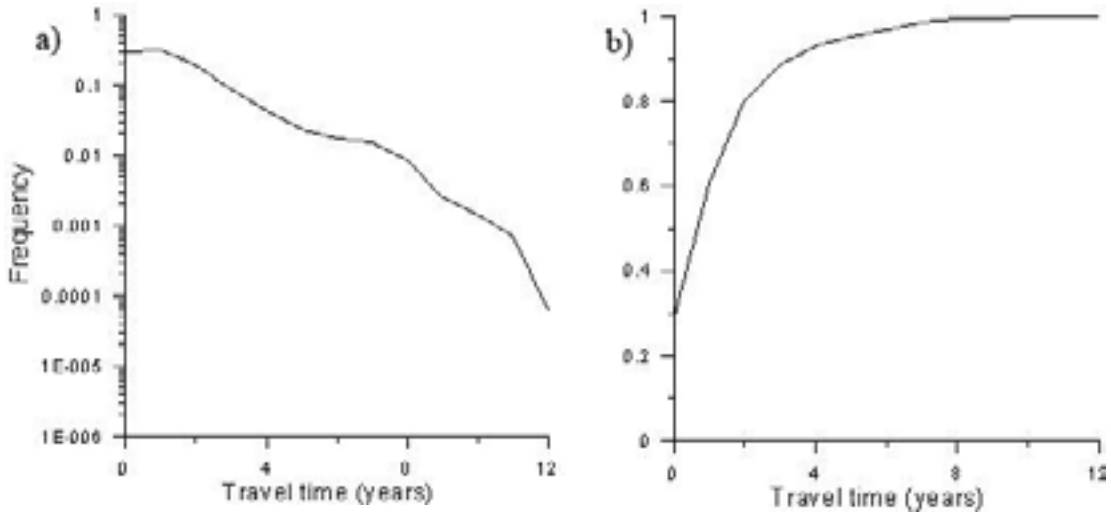

Figure 5-8. *Travel time distribution (a) and cumulative travel time distribution (b) to the surface water system for scenario II.*

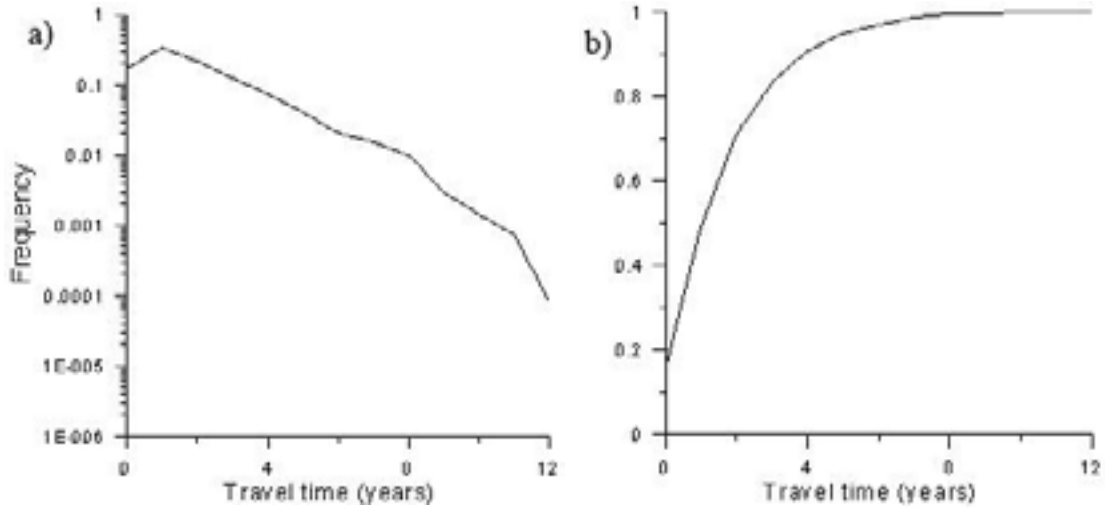

Figure 5-9. *Travel time distribution (a) and cumulative travel time distribution (b) from the area upstream of the surface water system to the coast for scenario II.*

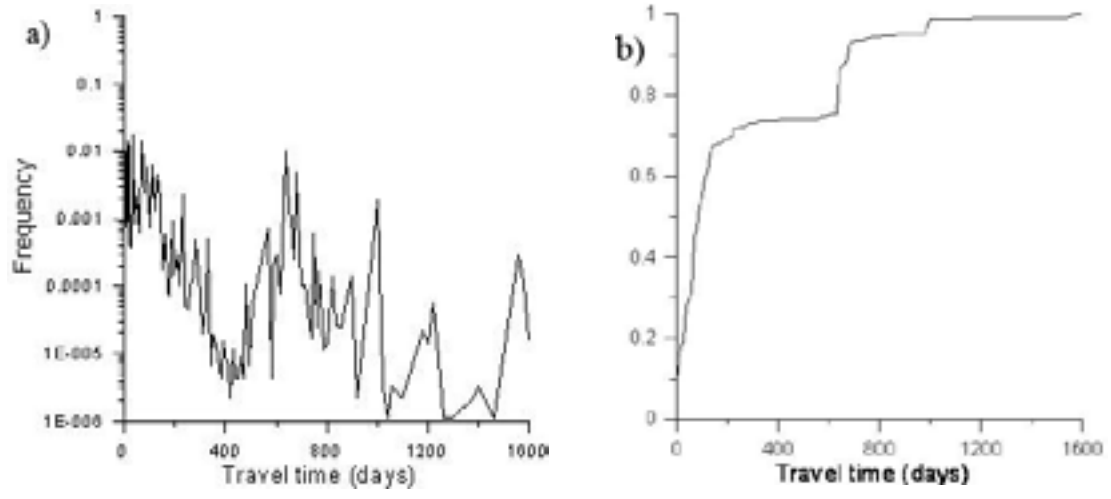

Figure 5-10. *Travel time distribution (a) and cumulative travel time distribution (b) from the pixels within the surface water systems (where β_{gw} = 0) to the coast.*

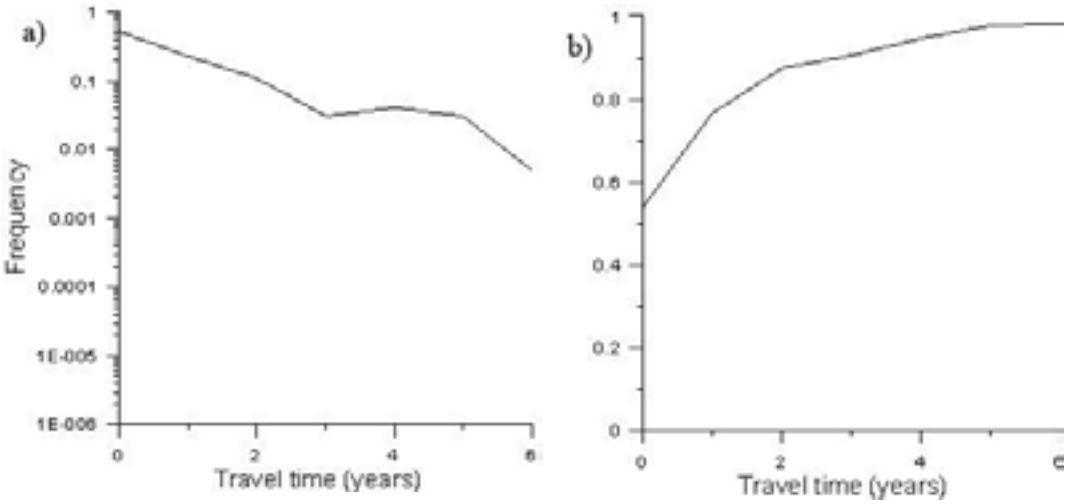

Figure 5-11. *Travel time distribution (a) and cumulative travel time distribution (b) from coastal sub-catchments where* $\gamma_{gw-s} = 0$ *(no surface water discharge into the sea) to the coast.*

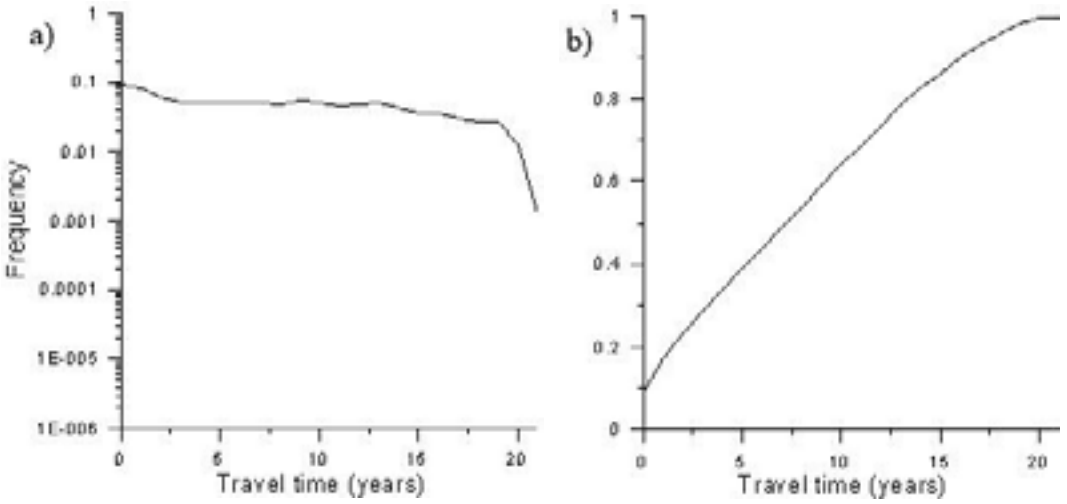

Figure 5-12. *Travel time distribution (a) and cumulative travel time distribution (b) to the coast for the entire model area considering scenario I.*

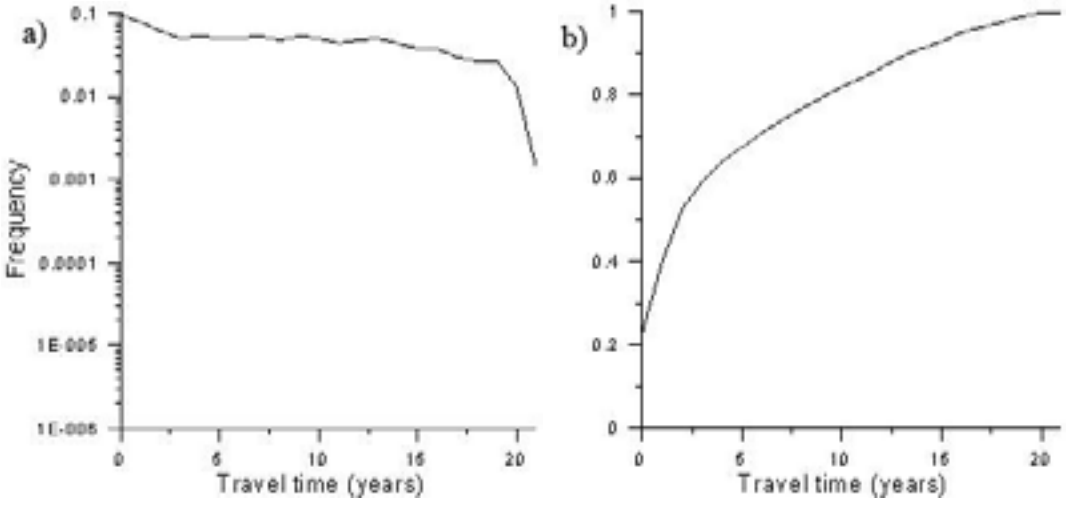

Figure 5-13. *Travel time distribution (a) and cumulative travel time distribution (b) to the coast for the entire model area considering scenario III.*

The total delivery factor of a solute which is assumed to be released uniformly throughout a specific area can be calculated as the mean of α in all the cells in that area. This average α can also be viewed as the expected delivery factor for a solute that is released at an unknown location somewhere in the area. If the total/average delivery factor is to be calculated by use of the Equations 2.5c–d, the advective travel time distributions shown in the Figures 5-8 to 5-13 correspond to the travel time pdfs. Total delivery factors for different attenuation rates are shown in Figure 5-16 and in Appendix 2.

The Figures 5-14 to 5-16 show that, for attenuation rates in the order $\lambda = 0.1–1$, the assumed transport pathway greatly impacts the solute delivery factor α from a large number of cells and, consequently, the average α for the whole the model area. However, it can be seen in Figure 5-16 that for low attenuation rate $\lambda \leq 0.01$/year, most of a released solute is likely to reach the sea in any transport pathway scenario (average $\alpha > 0.9$ in scenario I). For a rather high attenuation rate $\lambda = 10$/year, Figure 5-16 indicates that the delivery factor to the sea is significant only when the solute is released directly into surface water systems or into the Quaternary deposits-bedrock interface very close to the coast (e.g. in small coastal sub-catchments where $\gamma_{gw–s} = 0$). For even larger attenuation rate $\lambda \geq 100$/year, the average delivery factor is less than 0.1 even for release directly into surface water systems.

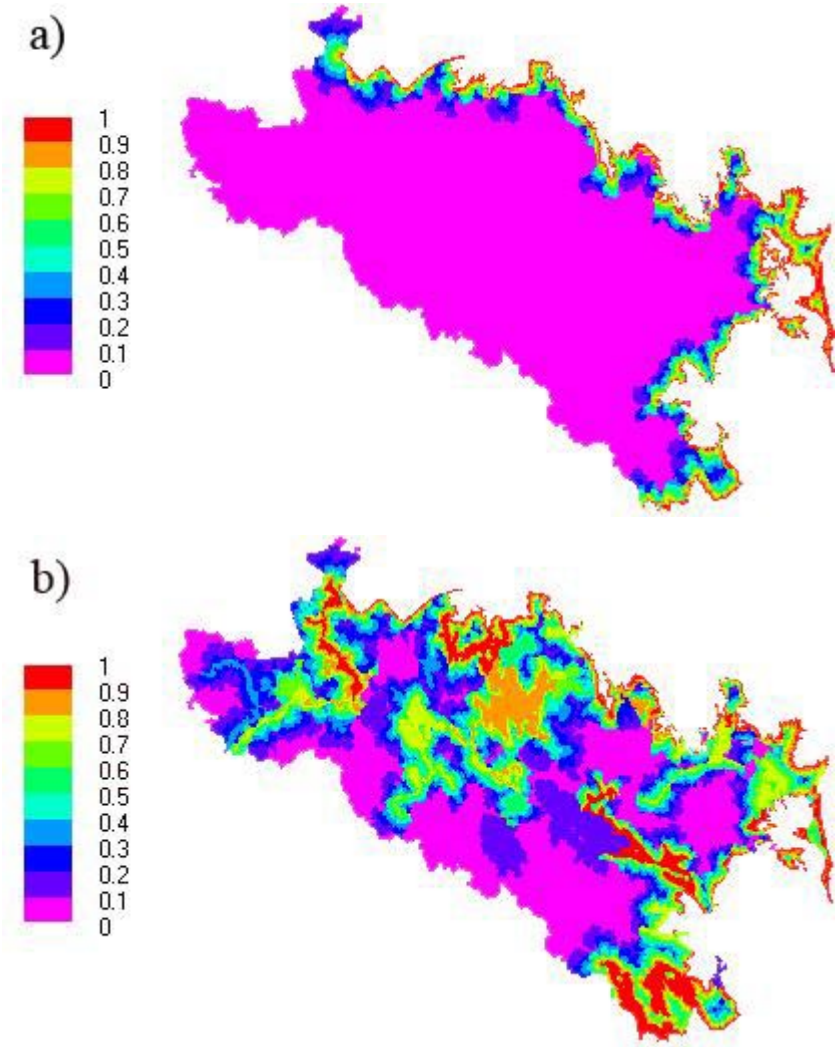

Figure 5-14. *Delivery factors for (a) scenario I and (b) scenario II, where $\lambda = 1$/year.*

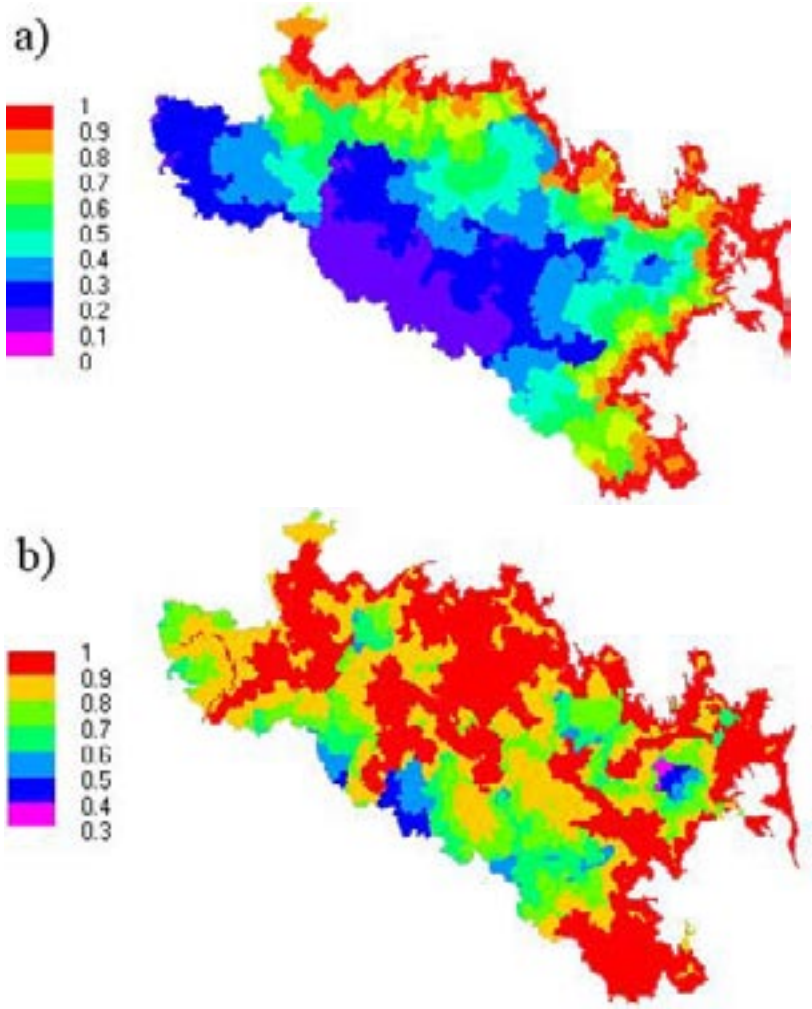

Figure 5-15. *Delivery factors for (a) scenario I and (b) scenario II, where λ = 0.1/year.*

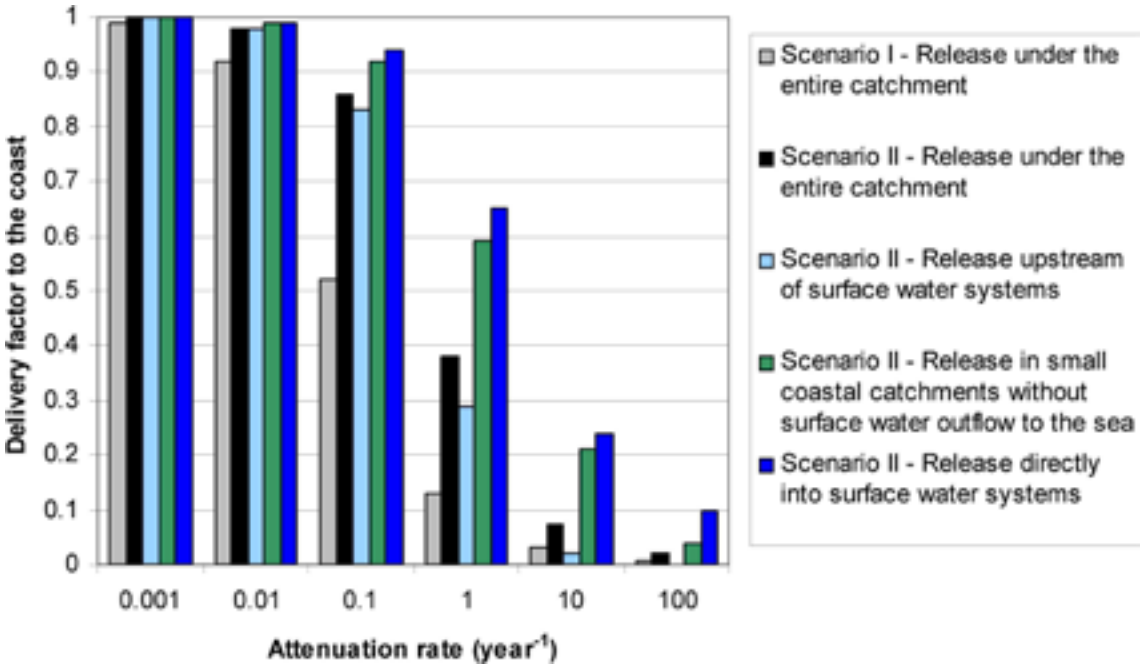

Figure 5-16. *Average delivery factors in different subareas considering different transport scenarios and attenuation rates.*

5.6 Uncertainty analysis

5.6.1 Effects of pathways through zones of near-stagnant groundwater

The above-used assumption of constant hydraulic gradient along individual streamlines may potentially lead to considerable overestimation of the groundwater flow velocity in very flat areas, particularly below lakes and wetlands. Therefore, we will in this section consider an alternative assumption, that flow along the considered pathways is governed by hydraulic gradients that equal the local (10×10 m grid) ground slope. "Old water" with high chloride content has been found below Lake Bolundsfjärden, Lake Eckarfjärden and Lake Gällsboträsket, which indeed indicates stagnant water below these lakes /Lindborg 2005/.

In order to assess the importance of the uncertainty in local hydraulic gradients, an alternative possible mean groundwater flow velocity has been calculated for each cell in the model as $v = K \cdot (slope)/n$, where *slope* is the mean ground slope in the cell. Hence, the hydraulic gradient is not constant along the streamlines in this case but equals the mean ground slope in each cell. An arbitrary value of 0.0001 is added to *slope* in the cells where $slope = 0$.

The resulting mean advective travel times in scenario I–II are shown in Figure 5-17. For scenario I, where flowpaths go in the Quaternary deposits-bedrock interface all the way out to the coast, the travel times are about two orders of magnitude longer for large parts of the model area than when constant hydraulic gradient is assumed in each individual catchment

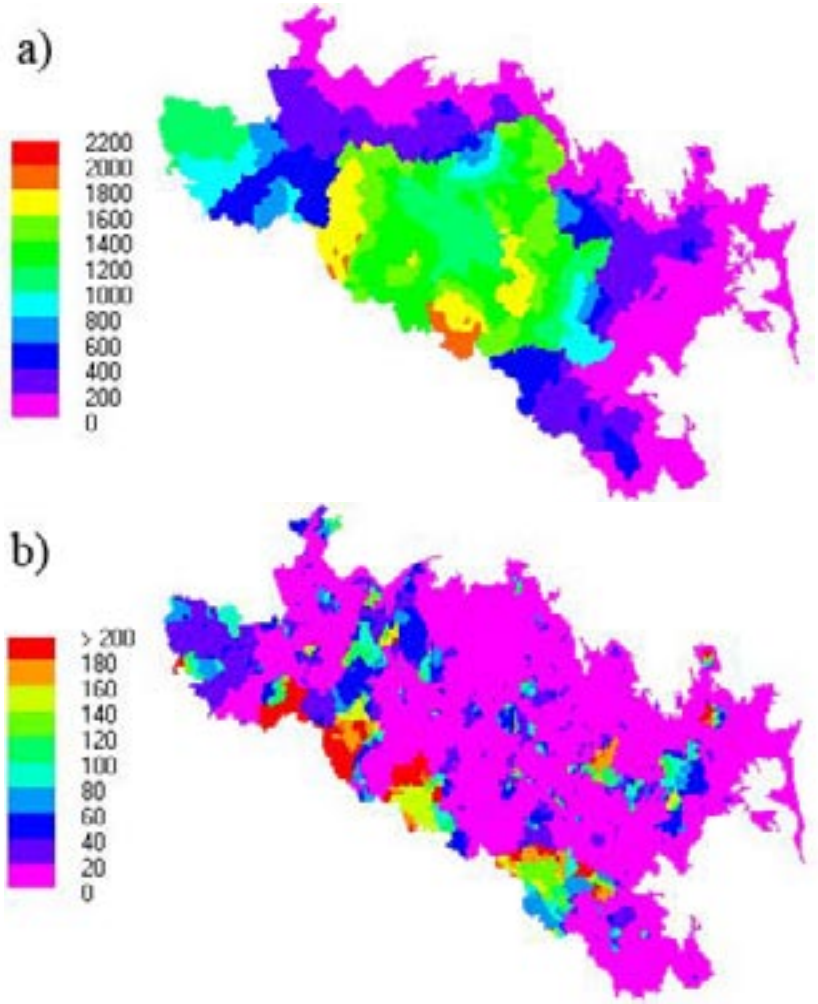

Figure 5-17. *Mean advective travel time (years) to the coast for (a) scenario I, and (b) scenario II, when the hydraulic gradient is assumed to equal the mean ground slope in each individual cell, except in the cells with zero mean slope where the hydraulic gradient is set to a value of 0.0001.*

(compare Figure 5-17a with Figure 5-7a). In scenario II, where the flow paths do not go below inland surface water, the assumption of variable hydraulic gradient along streamlines implies about one order of magnitude longer travel time for a large part of the area outside the surface water systems (compare Figure 5-17b with Figure 5-7b). The very long travel times when the hydraulic gradient is assumed to be equal to the local ground slope implies that the delivery factors of released solute may potentially be much lower than the ones presented in this report which then can be considered as conservative estimates.

5.6.2 Effects of travel time variability on estimated attenuation rates

Due to variability in flow length (due to e.g. various flow directions in flat terrain) and flow velocity (due to e.g. variable soil permeability), the solute travel time from a given location to the recipient can be expected to vary greatly between different flow paths. One input parameter that appears to be highly uncertain is the hydraulic conductivity. A constant value of $K = 1.5 \cdot 10^{-5}$ m/s was used in the calculation of the mean groundwater flow velocity for all cells in the model area, but the hydraulic conductivities obtained from hydraulic tests in the area varied over 5 orders of magnitude /Johansson et al. 2005/. If a 10 times higher value of the mean hydraulic conductivity is used instead, the transport through groundwater will be 10 times faster and the degradation rate need to be 10 times higher to result in the same attenuation along flow paths in groundwater. In addition, the travel times will also vary with time due to seasonal variability in precipitation and discharge that affect the hydraulic gradient.

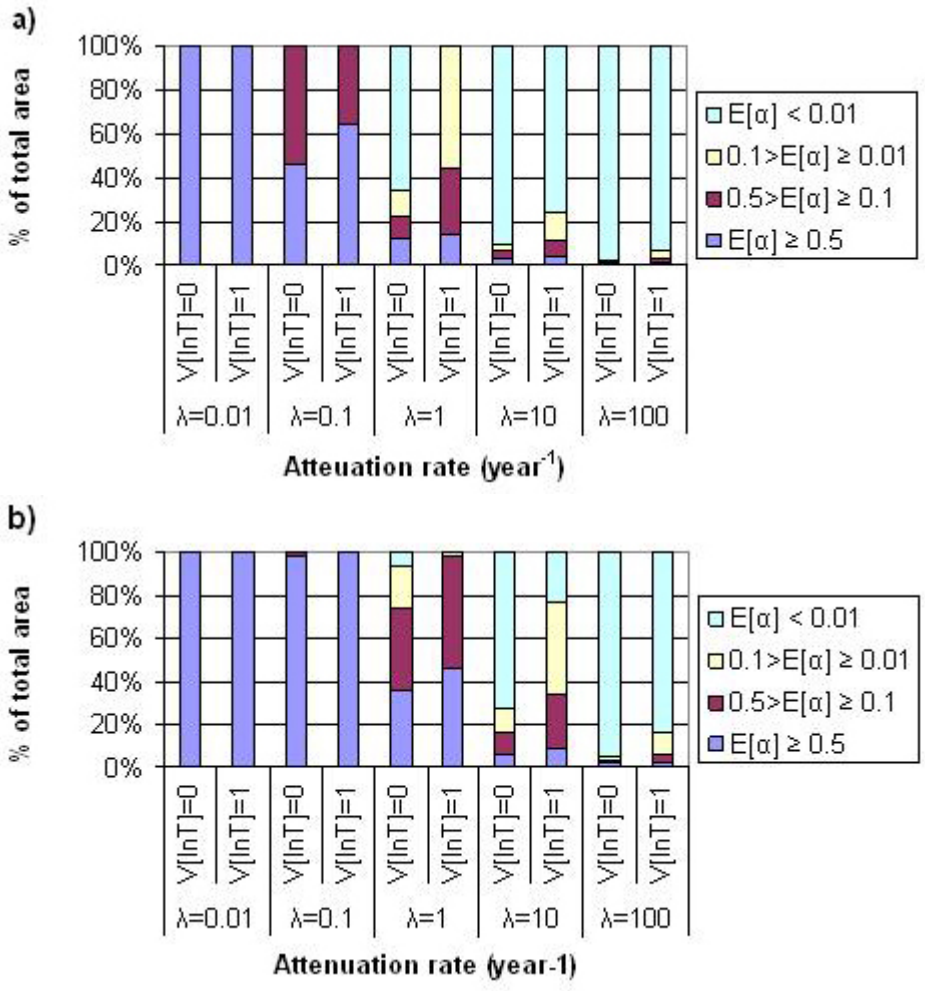

Figure 5-18. *Comparison of the percentage of total model area corresponding to different mean delivery factor intervals between homogeneous (V[lnT] = 0) and heterogeneous (V[lnT] = 1) conditions for (a) scenario I and (b) scenario II.*

In order to exemplify how travel time variability may affect model results, the travel time from each cell is assumed to be log-normally distributed around the previously calculated mean advective travel time. A rather high travel time variance of $V[\ln T] = 1$ is assumed in order to account for the undoubtedly large subsurface heterogeneity at the site and potentially large differences in the length of the flow paths from the same location. In order to calculate the expected values for the delivery factors for each cell, 100,000 Monte Carlo simulations are carried out (more than sufficient for stable simulation results). In each simulation, a travel time from each cell is generated randomly from the assumed log-normal distribution, and delivery factors are calculated according to the Equations 2.5c–d.

The expected value of the delivery factor from every one of the cells is calculated as the mean value of all simulations. Large travel time variance (e.g. $V[\ln T] = 1$) implies that the travel time to the recipient along many flow paths deviates significantly from the mean advective travel time. Attenuation along the fastest flow paths will of course be much lower than along flow paths where the transport time is close to the mean. The transport along fraction of flow paths with the longest travel time, on the other hand, does not affect mean delivery factors much if the mean advective travel time is already long enough to allow significant attenuation. As a result, travel time variability generally increases mean delivery factors. Figure 5-5 shows that the portion of the model area corresponding to relatively high mean delivery factors $E[\alpha]$ is considerably larger when travel time variability is accounted for.

In Figure 5-19 and Appendix 3, it is shown how travel time variability may affect the total α to the coast (i.e. the mean α in the entire model area) in scenario I and scenario II. Once again, the delivery factors in scenario III are the mean of the delivery factors in the other two scenarios. It can be seen in Figure 5-19 and Appendix 3 that the considered travel time variability does not increase the total/average α by more than factor 2 in any scenario. One can conclude that if the spatial distribution of mean travel time to the recipient can be estimated with reasonable accuracy, then expected mean delivery factors can also be quantified with reasonable accuracy for different attenuation rates even though the variance around the mean travel time is unknown.

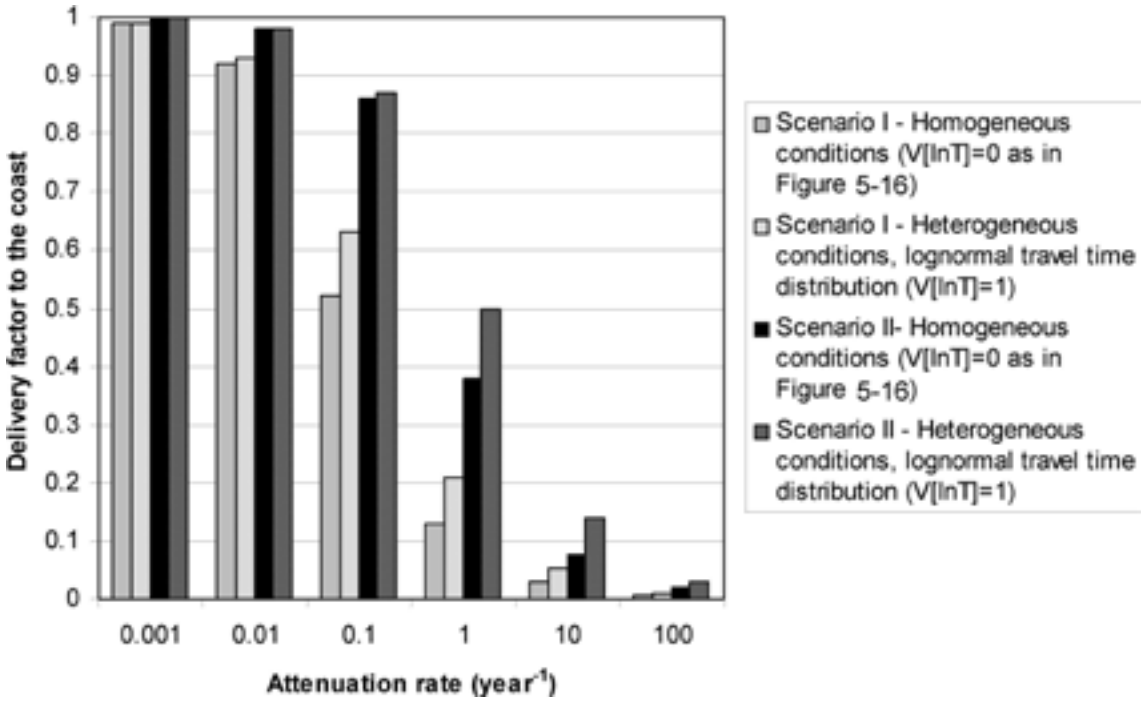

Figure 5-19. *The effect of travel time variability on average delivery factors considering different attenuation rates and transport scenarios.*

6 Knowledge gaps and recommendations

6.1 Theoretical conceptualisation

We formulate a general theoretical conceptualisation of solute transport from inland sources to downstream recipients, considering three main, distinctly different recipient load contributions from all different nutrient and pollutant sources that may exist within any catchment, namely load contributions from (i) all point source emissions directly into streams; (ii) all diffuse and point source mass inputs on the surface; and (iii) all diffuse and point source mass inputs in the subsurface. Specifically, considering these three main load contributions, we conceptually represent the water flow and waterborne mass transport and attenuation processes that govern any catchment area's nutrient and pollutant loading to its recipient.

As a basis, we use two main hydrological factors β_{gw} and $\gamma_{gw\text{–}s}$ that quantify the fraction of effective precipitation that recharges groundwater and the fraction of that subsurface recharge that contributes to stream flow, respectively, within the catchment area or model area. We further use mass delivery factors α that quantify the resulting relative nutrient/pollutant mass delivery into the recipient from the considered sources, noting that α may differ between different possible main transport pathways such as the stream network, the subsurface soil-groundwater system and the combined soil-groundwater and stream network system. Furthermore, α, β_{gw} and $\gamma_{gw\text{–}s}$ may be characteristic hydrological factors or functions for the whole catchment area or model area, or spatially dependent on the subareas associated with the different diffuse or point subsurface-related sources within the catchment.

Some of the above-mentioned source contributions – pathway combinations are commonly neglected in catchment-scale solute transport and attenuation modelling, in particular those related to subsurface sources, diffuse sources at the land surface and direct groundwater transport into the recipient. However, an important aspect of the here outlined theoretical conceptualisation is that it is model-independent. Its main hydrological factors, β_{gw} and $\gamma_{gw\text{–}s}$, and mass delivery factors α for different pathways can be quantified on the basis of inputs to and outputs from any considered model, either analytically or numerically (depending on the model used). Thereby, model performance and effects of underlying and often implicit model assumptions can be clarified, providing a tool for inter-model comparisons in SKB's site investigation or safety analysis programmes. Furthermore, since the parameters can, as previously mentioned, be defined for smaller (sub-)catchments of a specific recipient, we expect that the approach can also be used in analyses of specific ecosystem objects.

6.2 Groundwater discharge into recipients

The possible magnitude of the direct submarine groundwater discharge (SGD) and its importance as a transport pathway has been debated in the scientific literature /Moore 1996, Moore and Church 1996, Younger 1996, Li et al. 1999, Basu et al. 2001, Harvey 2002, Burnett et al. 2003, Destouni and Prieto 2003, Smith 2004, Prieto and Destouni 2005, Wilson 2005/, but may in any case be chemically and ecologically important for coastal waters, e.g. /Moore 1999, Burnett et al. 2003/. In addition, hydrogeochemical characteristics and pollution source loads may generally differ between larger, monitored catchments and smaller unmonitored coastal catchments, since for instance near-coastal areas are often characterised by relatively heavy population, special hydrogeochemical conditions and short transport pathways to the sea.

For instance, in addition to a relatively high variability of key chemical parameters (e.g. pH and dissolved organic carbon) between small (< 15 km^2) unmonitored Swedish catchments reported in /Temnerud and Bishop 2005/, the near-coastal transition zones of brackish groundwater between seawater and fresh groundwater may also contribute to general differences in the

hydrogeochemical conditions (in parts of) of coastal catchments as compared to inland catchments. Realistic quantification of how near-coastal diffuse groundwater flows interact and combine with the surface water flows to feed freshwater and waterborne substances from land to sea is necessary for relevant coastal load estimates.

Such quantification and modelling efforts may currently be hampered by hydrological data gaps in systematically unmonitored near-coastal catchment areas (see, e.g. /Hannerz and Destouni 2006/ for the Baltic Sea coast example). This emphasises the importance of extending in time the recently started hydrological and hydrogeochemical data series in the Forsmark and Simpevarp coastal catchment areas, since they are in effect unmonitored from a hydrological viewpoint, due to the lack of extended discharge time series.

6.3 Demonstration analyses of solute transport in Forsmark

In order to further clarify and explain research questions that may be of particular importance for transport pathways from deep groundwater surrounding a repository and the relation between, on the one hand, (deep) subsurface source distributions and extents, and on the other hand, resulting solute distributions in the shallow water system, we here performed an initial demonstration analysis of solute transport through coupled ground-surface-coastal water systems of Forsmark. We thereby concretise and interpret some selected transport scenarios for model conditions in the Forsmark catchment area (see, e.g. /Jarsjö et al. 2004, 2006/). In order to quantify the model-independent key hydrological and mass delivery factors of the general theoretical conceptualisation, we used transport-decay modelling by use of the PCRaster-approach /van Deursen 1995, Darracq et al. 2005, Darracq and Destouni 2005/. The results were expressed in terms of groundwater and surface water travel time distributions for different possible investigation scenarios with the mass delivery factors calculated analytically using Equations 2.5c–d.

Before performing the above-mentioned transport scenario analyses, we further investigated possible uncertainties in predicted coastal discharges due to uncertain spatial variation of evapotranspiration within the catchment, since such flow uncertainties influences subsequent transport quantifications. Results showed that the spatial distribution of local precipitation surplus (PS; precipitation minus evapotranspiration, equalling the locally created runoff) can be largely influenced by small-scale variability in evapotranspiration, as governed by local vegetation, soil texture and land-use details. However, even for the relatively small catchment sizes considered here, the relatively large, focused surface water discharges from land to sea were essentially unaffected by the spatial variability and uncertainty in local PS, because local PS differences were averaged out along the length of the main water flow paths.

In contrast, local flux values within the diffuse groundwater flow field from land to sea are generally characterised by shorter flowpaths and are therefore more affected by the spatial variability of local PS. This implies that spatial modelling uncertainties are the largest for the relatively small local flux values within diffuse SGD fields, for which the full variability range can also not be readily and fully observed through direct measurement. Nevertheless, in consistency with results from previous totally independent and different (cross-sectional groundwater focused, rather than the present catchment-area and surface water focused) approaches to SGD quantification /Destouni and Prieto 2003, Prieto et al. 2006/, the present results indicate that mean values and total sums of SGD along some considerable coastline length, based on catchment-scale hydrological balance constraints, may be robust and considerably more certain than the modelling of the spatially variable small local fluxes within diffuse SGD fields.

Regarding site-specific estimates of such total magnitude of SGD, the here reported results and /Jarsjö et al. 2004, 2006/ showed that, for both the Forsmark and Simpevarp areas, 80% to 90% of the total coastal discharge occurred through focused flows in visible streams, whereas the remaining 10% to 20% was diffuse and occurring through submarine groundwater discharge (SGD), small transient streams, or both, at different points in time.

In the performed initial demonstration analysis of solute transport pathways from deep groundwater to recipients at the surface, we considered the two main scenarios: (I) transport in the Quaternary deposits-bedrock interface zone only (hence assuming that the deep groundwater transport pathway to the coast does not include the surface water system), and (II) transport in the coupled groundwater-surface water system (a third scenario was also considered, where half of the solute is transported as in scenario I, and half as in scenario II).

Considering mean travel times from each model cell to the coast, and disregarding travel times in the deep bedrock domain itself (which may be added to the here presented values), results show that travel times in scenario (II) were less than 4 years in 90% of the considered model area (i.e. the Forsmark catchment area). Travel times were longer in scenario (I) with values higher than 10 years in 40% of the catchment area. These results are based on the assumption that the pathways do not go through zones of near-stagnant groundwater (found e.g. below Lake Bolundsfjärden, Lake Eckarfjärden and Lake Gällsboträsket in Forsmark). If they would do so (and the above assumption is violated), results show that travel times can be considerably longer, for instance exceeding 400 years in half of the model area in scenario (I).

Furthermore, travel time distributions were estimated on the basis of frequencies of these spatially distributed travel times, considering the entire catchment as well as specific regions of interest. For instance, we considered travel times to the coast in small coastal catchments without permanent streams, as well as travel times to surface water systems from upstream regions, leading in the latter case to practically identical travel times as those to the coast for the coupled groundwater-surface water system, due to the relatively short travel times in surface water systems. Generally, such travel time distributions may either be interpreted in a deterministic sense, as the actual travel times from a diffuse source entering the entire considered region, or in a probabilistic sense, as a travel time probability density function (pdf) for a particle that is equally likely to enter any point of the considered area.

Considering now attenuation (caused by e.g. biogeochemical reactions or decay) along the hydrological transport pathways to inland surface waters and to the coast, we estimate delivery factors, representing the fraction of solute mass released in a model cell that reaches the considered recipient. Results showed that average delivery factors, representing the whole catchment and equalling expected delivery factors in the probabilistic case, can exhibit considerable differences between transport pathway scenarios (I) and (II). For instance, for attenuation rates λ around 0.1 year^{-1}, about 50% of the mass entering the Quaternary deposits will reach the coast in scenario (I), whereas almost 90% will reach the coast in scenario (II), where travel times are shorter. Also, results can differ considerably depending on the considered (sub)area. For scenario (II) and λ = 1 year^{-1}, for instance, about 30% of the mass released upstream of the surface water systems will reach the coast, whereas as much as 65% of the mass released directly into the surface water systems will reach the coast.

However, the magnitude of the differences in average delivery factors (between transport pathway scenarios as well as between considered release points) depends on the actual λ-values. This exemplified for the Forsmark area in Figure 6-1, where λ is shown on the x-axis and differences in average delivery factors between different cases are shown on the y-axis. For instance, for $\lambda < 0.01$ year^{-1} there is a relatively small difference (~1% or less) in delivery factor between contaminants released in the surface water systems and upstream of the surface water systems (pink curve in Figure 6-1), whereas the difference in this case reaches a maximum of ~35% for λ = 1 year^{-1} (approximately). This is because for low λ's, practically all mass reaches the coast regardless of release point. For high λ's, only a small fraction of the mass reaches the coast regardless of release point. Note however, that for high λ's, the relative differences in delivery factors between different scenarios may be large although the absolute differences are small, which is not the case for low λ's.

The above results imply that, in general, mass delivery factors to recipients are sensitive to both pathways and entrance points or areas in the Quaternary deposits of Forsmark, with for instance a remaining key question being to which extent the deep groundwater transport pathway to the coast includes the surface water system and/or Quaternary deposits-bedrock interface zone.

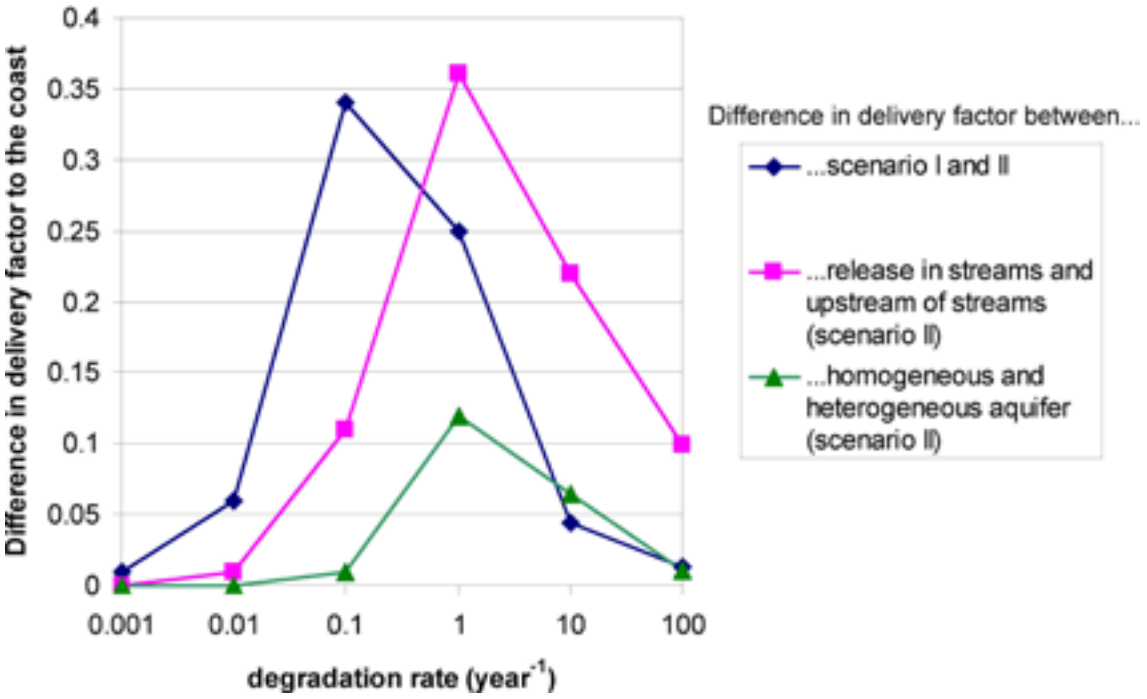

Figure 6-1. *Difference in estimated delivery factors to the coast between main transport scenarios as a function of the attenuation rate λ.*

However, given more specific sub-catchment areas (e.g. of biosphere objects of interest) and possible ranges of attenuation rates (of compounds of interest) from parallel studies, the present analyses also show that robust predictions regarding e.g. mass delivery can in some cases be obtained despite considerable pathway and entrance point uncertainties.

Because such cases then can be excluded from further investigation, it appears that specific transport analyses that consider relevant combinations of possible release points, transport pathway scenarios and attenuation rates can be used for delimiting specific priority regions, where remaining uncertainties are high and further experimental investigations and/or monitoring hence may be needed to reduce the uncertainties.

As for modelling approaches in addition to those already mentioned, Monte Carlo simulations may prove useful within the presented framework, for investigating effects of parameter uncertainty. An example is given here for the case of uncertain aquifer travel times, in which 100.000 realisations of possible travel time variability were obtained and combined with a deterministic model of travel times in the surface water systems. Although the results were only presented in terms of the average travel times for all realisations (or travel time differences as compared to a homogeneous aquifer, shown by the green curve in Figure 6-1), we note that the large number of realisations also means that one can estimate confidence limits for such predictions.

7 Conclusion summary

The conclusions of the present work can be summarised as follows:

- The here formulated, model-independent conceptual framework for solute transport from inland sources to downstream recipients provides a possible tool for clarification of underlying and often implicit model assumptions, which can be useful for e.g. inter-model comparisons in SKB's site investigation or safety analysis programmes.
- National hydrological monitoring data systematically exclude smaller, coastal catchments, which are known to differ from larger, monitored catchments e.g. in population density, hydrogeochemical conditions and solute transport pathway lengths. This emphasises the importance of extending in time the recently started hydrological and hydrogeochemical data series in the Forsmark and Simpevarp coastal catchment areas, which presently lack extended discharge time series.
- Performing an initial demonstration analysis of the Forsmark area, and considering possible solute attenuation (caused by e.g. biogeochemical reactions or decay) along the hydrological transport pathways to inland surface waters and to the coast, we estimate mass delivery factors representing the fraction of solute mass released in a model cell that reaches the considered recipient. Results show that average delivery factors, representing the whole catchment, can exhibit considerable differences between the possible transport scenarios I (transport in the Quaternary deposits-bedrock interface zone only) and II (transport in the coupled groundwater-surface water system).
- The magnitude of the above-mentioned differences in average delivery factors between different possible transport scenarios, as well as between different possible solute release locations, depends on the prevailing attenuation rate λ. This is because for low λ's ($\lambda < 0.01$ year^{-1} considering both scenarios and the entire Forsmark area), practically all solute mass reaches the coast regardless of release location and scenario, and for high λ's ($\lambda > 10$ year^{-1} considering both scenarios and the entire Forsmark area) only a small fraction of the released solute mass reaches the coast regardless of release location and scenario.
- The results generally imply that resulting solute mass delivery to recipients is sensitive to both solute transport pathways and solute entrance locations (or areas) in the Quaternary deposits of Forsmark. Zones of near-stagnant groundwater that have been found below three lakes in the Forsmark area may considerably prolong transport times in some cases. In particular, key issues and recommended ways for addressing the issues are:
  - *investigating to which extent the deep groundwater transport pathway to the coast includes predominantly the surface water system, or predominantly the Quaternary deposits-bedrock interface zone, or a considerable combination of both*. There is a need for a relatively broad assessment study, identifying which methods, modelling and measurement results are needed to answer the question.
  - *delimiting of "low-uncertainty" cases, for which further investigations would not be of highest priority*. This can be obtained through carrying out more detailed transport simulation analyses considering relevant combinations of possible solute release locations, transport pathway scenarios and attenuation rates. By analogy, simulation studies should also be used for *delimiting cases where remaining uncertainties are high* and further experimental/field investigations and/or monitoring is needed to reduce the uncertainties to manageable levels. Such simulation studies could be separate or constitute a part of the above-mentioned assessment study.

References

Anderson M P, 2005. Heat as a groundwater tracer. Ground Water, 43, 951–968.

Avila R M, Kautsky U, Ekström P A, 2006. Modeling the long-term transport and accumulation of radionuclides in the landscape for derivation of dose conversion factors. Ambio, 35, 513–523.

Baresel C, Destouni G, 2005. Novel quantification of coupled natural and cross-sectoral water and nutrient/pollutant flows for environmental management Environmental Science and Technology 39, 6182–6190.

Basu A R, Jacobsen S B, Poreda R J, Dowling C B, Aggarwal P K, 2001. Large groundwater strontium flux to the oceans from the Bengal Basin and the marine strontium isotope record. Science, 293, 1470–1473.

Bauer S, Beyer C, Kolditz O, 2006. Assessing measurement uncertainty of first-order degradation rates in heterogeneous aquifers. Water Resources Research, 42, W01420, doi:10.1029/2004WR003878.

Bayer-Raich M, Jarsjö J, Liedl R, Ptak T, Teutsch G, 2006. Integral pumping test analyses of linearly sorbed groundwater contaminants using multiple wells: Inferring mass flows and natural attenuation rates. Water Resources Research, 42, W08411, doi:10.1029/2005WR004244.

Beinhorn M, 2005. Contributions to computational hydrology. Non-linear flow processes in subsurface and surface hydrosystems. PhD thesis. Center for Applied Geosciences, University of Tübingen, Tübingen (http://w210.ub.uni-tuebingen.de/dbt/volltexte/2005/2022/pdf/Diss_Beinhorn_TGA90.pdf).

Bokuniewicz H J, 1992. Analytical descriptions of subaqueous groundwater seepage. Estuaries, 15: 458–464.

Boresjö Bronge L, Wester K, 2002. Vegetation mapping with satellite data of the Forsmark and Tierp regions. SKB R-02-06, Svensk Kärnbränslehantering AB.

Boresjö Bronge L, Wester K, 2003. Vegetation mapping with satellite data of the Forsmark, Tierp and Oskarshamn regions. SKB P-03-83, Svensk Kärnbränslehantering AB.

Brunberg A-K, Carlsson T, Blomqvist P, Brydsten L, Strömgren M, 2004. Identification of catchments, lake-related drainage parameters and lake habitats, SKB P-04-25, Svensk Kärnbränslehantering AB.

Brydsten L, 2004. A method for construction of digital elevation models for site investigation program in Forsmark and Simpevarp. SKB P-04-03, Svensk Kärnbränslehantering AB.

Brydsten L, Strömgren M, 2004. Digital elevation models for the site investigation programme in Forsmark. Site description version 1.2. SKB R-04-70, Svensk Kärnbränslehantering AB.

Burnett W C, Taniguchi M, Oberdorfer J, 2001. Measurement and significance of the direct discharge of groundwater into the coastal zone. J. Sea Res., 46: 109-116.

Burnett W C, Bokuniewicz H, Huettel M, Moore W S, Taniguchi M, 2003. Groundwater and pore water inputs to the coastal zone. Biogeochemistry, 66, 3–33.

Burnett W C et al. 2006. Quantifying submarine groundwater discharge in the coastal zone via multiple methods. Science of the total Environment, 367: 498–543.

Buscheck T E, Alcantar C M, 1995. Regression techniques and analytical solutions to demonstrate intrinsic bioremediation, in Intrinsic Bioremediation, edited by R. E. Hinchee, T. J. Wilson, and D. Downey, pp. 109– 116, Battelle Press, Columbus, Ohio.

Cartwright K, 1970. Groundwater discharge in the Illinois basin as suggested by temperature anomalies. Water Resour. Res. 6(3): 912–918.

Conant B, 2004. Delineating and quantifying ground water discharge zones using streambed temperatures. Ground Water, 42(2): 243–257.

Darracq A, Destouni G, 2005. In-stream nitrogen attenuation: Model-aggregation effects and implications for coastal nitrogen impacts. Environmental Science and Technology, 39, 3716–3722.

Darracq A, Greffe F, Hannerz F, Destouni G, Cvetkovic V, 2005. Nutrient transport scenarios in a changing Stockholm and Malaren valley region, Sweden. Water Science and Technology 51,: 31–38.

De Jonge J, 2005. Contributions to computational geotechnics. Non-isothermal flow in low-permeable porous media. PhD thesis. Center for Applied Geosciences, University of Tübingen, Tübingen.

Destouni G, Prieto C, 2003. On the possibility for generic modeling of submarine groundwater discharge. Biogeochemistry, 66: 171–186.

Destouni G, Gren I M, 2005. Response to 'Discussion of the paper "Cost effective policies for alternative distributions of stochastic water pollution" by Gren, Destouni and Tempone' by Karnpas and Adarnidis. Journal of Environmental Management, 74, 389–392.

Destouni G, Darracq A, 2006. Response to comment on "In-stream nitrogen attenuation: Model-aggregation effects and implications for coastal nitrogen impacts" Environmental Science and Technology, 40, 2487–2488.

Destouni G, Hannerz F, Jarsjö J, Prieto C, Shibuo Y, 2008. Small unmonitored areas yielding large waterborne substance loads from land to sea, Global Biogeochemical Cycles (in review).

De Wit M J M, 1999. Nutrient fluxes in the Rhine and Elbe basins. Ph.D. Thesis, Utrecht University, the Netherlands, NGS Publication 259, 163 pp.

De Wit M J M, 2001. Nutrient fluxes at the river basin scale. I: the PolFlow model. Hydrological Processes, 15, 743–759.

DHI, 2007. MIKE SHE Additional modules. Internet page: http://www.dhigroup.com/Software/WaterResources/MIKESHE/Details/AdditionalModules.aspx, visited 2008-01-21.

Diersch H-JG, 1996. Interactive, graphics-based finite-element simulation system FEFLOW for modelling groundwater flow, contaminant mass and heat transport processes. User's Manual Version 4.6. WASY, Institute for Water Resources Planning and System Research Ltd, Berlin.

Falta R W, Rao P S, Basu N, 2005. Assessing the impacts of partial mass depletion in DNAPL source zones – I. Analytical modeling of source strength functions and plume response. Journal of Contaminant Hydrology 78, 259–280.

Fredriksson D, 2004. Peatland investigation Forsmark. SKB P-04-127, Svensk Kärnbränslehantering AB.

Freeze R A, Cherry J A, 1979. Groundwater. Prentice-Hall Inc., Englewood Cliffs, NJ, 604 p.

Fukuo Y, Kaihotsu I, 1988. A theoretical analysis of seepage flow of the confined groundwater into the lake bottom with a gentle slope. Water Resour. Res., 24: 1949–1953.

Genereux D P, Wood S J, Pringle C M, 2002. Chemical tracing of interbasin groundwater transfer in the lowland rainforest of Costa Rica. Journal of Hydrology, 258: 163–178.

Graham D N, Butts M B, 2005. Flexible, integrated watershed modelling with MIKE SHE. In Watershed Models, Eds. V P Singh & D K Frevert Pages 245–272, CRC Press. ISBN: 0849336090 (Available at http://www.dhigroup.com/Software/Download/DocumentsAndTools/PapersAndDocs/WaterResources.aspx).

Grip H, Rodhe A, 2000. Vattnets väg från regn till back. Hallgren & Fallgren, Uppsala. (In Swedish.)

Haitjema H M, 1995. Analytic element modeling of groundwater flow. San Diego, California, Academic Press.

Hannerz F, Destouni G, 2006. Spatial characterization of the Baltic Sea Drainage Basin and its unmonitored catchments. AMBIO, 214–219.

Harvey C F, 2002. Groundwater flow in the Ganges Delta. Science, 296, 1563A.

Hunt R J, Haitjema H M, Krohelski J T, Feinstein D T, 2003. Simulating ground water-lakes interactions: Approaches and insights. Ground Water, 41(2): 227–237.

Hydrogeologic Inc, 2003. MODHMS software (Version 2.0) documentation. Volume I: groundwater flow modules, Volume II: Transport modules, Volume III: Surface water flow modules, Herndon, USA.

Jarsjö J, Shibuo Y, Destouni G, 2004. Using the PCRaster-POLFLOW approach to GIS-based modelling of coupled groundwater-surface water hydrology in the Forsmark Area. SKB R-04-54, Svensk Kärnbränslehantering AB.

Jarsjö J, Bayer-Raich M, Ptak T, 2005. Monitoring groundwater contamination and delineating source zones at industrial sites: Uncertainty analyses using integral pumping tests. Journal of Contaminant Hydrology, 79, 107–134.

Jarsjö J, Shibuo Y, Prieto C, Destouni G, 2006. GIS-based modelling of coupled groundwater – surface water hydrology in the Forsmark and Simpevarp areas. SKB R-05-67, Svensk Kärnbränslehantering AB.

Jarsjö J, Bayer-Raich M, 2008. Estimating plume degradation rates in aquifers: Effect of propagating measurement and methodological errors. Water Resources Research, 44, W02501, doi:10.1029/2006WR005568.

Jarsjö J, Shibuo Y, Destouni G, 2008. Spatial distribution of unmonitored inland water flows to the sea. Journal of Hydrology, vol. 348, 59–72, doi: 10.1016/j.jhydrol.2007.09.052.

Jobson H E, Harbaugh A W, 1999. Modifications to the diffusion analogy surface-water flow model (DAFLOW) for coupling to the modular finite-difference ground-water flow model (MODFLOW). Open-file Report 99–217, USGS.

Johansson P-O, 2003. Drilling and sampling in soil. Installation of groundwater monitoring wells and surface water level gauges. SKB P-03-64, Svensk Kärnbränslehantering AB.

Johansson P-O, Werner K, Bosson E, Juston J, 2005. Description of climate, surface hydrology, and near-surface hydrology. Preliminary site description. Forsmark area – version 1.2. SKB R-05-06, Svensk Kärnbränslehantering AB.

Kalbus E, Reinstorf F, Schirmer M, 2006. Measuring methods for groundwater – surface water interactions: a review. Hydrology and Earth System Sciences, 10(6): 873–887.

Kaleris V, Lagas G, Marczinek S, Piotrowski J A, 2002. Modelling submarine groundwater discharge: an example from the western Baltic Sea. Journal of Hydrology, 265: 76–99.

Karpen V, Thomsen L, Suess E, 2006. Groundwater discharges in the Baltic Sea: survey and quantification using a schlieren technique application. Geofluids, 6: 241–250.

Kavanaugh M C et al. 2003. The DNAPL remediation challenge: is there a case for source depletion? Expert panel report EPA/600/R-03/143, Natl. Risk Manage. Res. Lab., U.S. Environ. Prot. Agency, Cincinnati, Ohio,USA.

Kolditz O et al. 2006a. GeoSys/RockFlow Version 4.3.21(WW) Open Source Software Design Proposal. August 2006.

Kolditz O et al. 2006b. High performance computing in applied geosciences. GeoSys-Preprint [2006-26]. Center for Applied Geosciences, University of Tübingen (http://www.unituebingen.de/zag/geohydrology/index.html?literature/reports/literature.html).

Konikow L F, Goode D J, Hornberger G Z, 1996. A Three-Dimensional Method-of-Characteristics Solute-Transport Model (MOC3D): U.S. Geological Survey Water-Resources Investigations Report 96-4267, 87 p.

Kooi H, Groen J, 2001. Offshore continuation of coastal groundwater systems; predictions using sharp-interface approximations and variable-density flow modelling. Journal of Hydrology, 246: 19–35.

Kraemer T F, 2005. Radium isotopes in Cayuga Lake, New York: Indicators of inflow and mixing processes. Limnol. Oceanogr., 50(1): 158–168.

Krupa S L, Belanger T V, Heck H H, Brok J T, Jones B J, 1998. Krupaseep – the next generation seepage meter. J. Coast. Res., 25: 210–213.

Langevin C D, Swain E, Wolfert M, 2005. Simulation of integrated surface-water/ground-water flow and salinity for a coastal wetland and adjacent estuary. Journal of Hydrology, 314: 212–234.

Larsson-McCann S, Karlsson A, Nord M, Sjögren J, Johansson L, Ivarsson M, Kindell S, 2002. Meteorological, hydrological and oceanographical data for the site investigation program in the communities of Östhammar and Tierp in the northern part of Uppland. SKB TR-02-02, Svensk Kärnbränslehantering AB.

Lee D R, 1977. Device for measuring seepage flux in lakes and estuaries. Limnol. Oceanogr., 22(1): 140–147.

Li K B, Goovaerts P, Abriola L M, 2007. A geostatistical approach for quantification of contaminant mass discharge uncertainty using multilevel sampler measurements. Water Resources Research, 43, W06436, doi:10.1029/2006WR005427.

Li L, Barry D A, Stagnitti F, Parlange J-Y, 1999. Submarine groundwater discharge and associated chemical input to a coastal sea. Water Resources Research, 35, 3253–3259.

Lindborg T (editor), 2005. Description of surface systems. Preliminary site description Forsmark area – version 1.2. SKB R-05-03, Svensk Kärnbränslehantering AB.

Lindborg T (editor), 2006. Description of surface systems. Preliminary site description Laxemar subarea – version 1.2. SKB R-06-11, Svensk Kärnbränslehantering AB.

Lindborg T, Lindborg R, Löfgren A, Söderbäck B, Bradshaw C, Kautsky U, 2006. A strategy for describing the biosphere at candidate sites for repositories of nuclear waste: Linking ecosystem and landscape modeling. Ambio 35, 418-424.

Lindgren G A, Destouni G, 2004. Nitrogen loss rates in streams: Scale-dependence and up-scaling methodology Geophysical Research Letters 31, Art. No. L13501.

McBride M S, Pfannkuch H O, 1975. The distribution of seepage within lakebed. J. Res. U.S. Geol. Surv., 3: 505–512.

McDonald M G, Harbaugh A W, 1988. A modular three-dimensional finite-difference ground-water flow model. Techniques of Water-Resources Investigations, Book 6, Chap A1, USGS.

Malmström M E, Destouni G, Banwart S A, Strömberg B H E, 2000. Resolving the scale-dependence of mineral weathering rates. Environmental Science and Technology, 34, 1375–1378.

Malmström M E, Destouni G, Martinet P, 2004. Modeling expected solute concentration in randomly heterogeneous flow systems with multicomponent reactions. Environmental Science and Technology, 38, 2673–2679.

Malmström M E, Berglund S, Jarsjö J, 2008. Combined effects of spatially variable flow and mineralogy on the attenuation of acid mine drainage in groundwater. Applied Geochemistry, 23, 1419–1436, doi: 10.1016/j.apgeochem.2007.12.029.

Moore W S, 1996. Large groundwater inputs to coastal waters revealed by 226Ra enrichments. Nature, 380, 612–614.

Moore W S, Church T M, 1996. Submarine groundwater discharge – Reply. Nature 382, 122-122.

Moore W S, 1999. The subterranean estuary: a reaction zone of ground water and sea water. Marine Chemistry 65 (1–2), 111–125.

Nilsson A-C, Borgiel M, 2004. Sampling and analyses of surface waters. Results from sampling in the Forsmark area, March 2003 to March 2004. SKB P-04-146, Svensk Kärnbränslehantering AB.

Niswonger R G, Prudic D E, 2005. Documentation of the Streamflow-Routing (SFR2) Package to Include Unsaturated Flow Beneath Streams – A Modification to SFR1. U.S. Geological Survey Techniques and Methods 6-A13, 48 p.

Oberdorfer J, 2003. Hydrogeologic modeling of submarine groundwater discharge: comparison to other quantitative methods. Biogeochemistry, 66: 159–169.

Panday S, Huyarkon P S, 2004. A fully coupled physically-based spatially-distributed model for evaluating surface/subsurface flow. Advances in Water Resources, 27: 361–382.

Paulsen, R J, Smith C F, O'Rourke D, Wong T F, 2001. Development and evaluation of an ultrasonic ground water seepage meter. Ground Water, 39(6): 904–911.

Piekarek-Jankowska H, 1996. Hydrochemical effects of submarine groundwater discharge to the Puck Bay (Southern Baltic Sea, Poland). Geographia Polonica, 67: 103–119.

Prieto C, Destouni G, 2005. Quantifying hydrological and tidal influences on groundwater discharges into coastal waters. Water Resources Research 41, Art. No. W12427.

Prieto C, Kotronarou A, Destouni G, 2006. The influence of temporal hydrological randomness on seawater intrusion in coastal aquifers. Journal of Hydrology, 330, 285–300.

Prudic D E, 1989. Documentation of a computer program to simulate stream–aquifer relations using a modular, finite-difference, ground-water flow model. Open-File Report 88-729, USGS.

Prudic D E, Konikow L F, Banta E R, 2004. A new streamflow-routing (SFR1) package to simulate stream-aquifer interaction with MODFLOW-2000. U.S. Geological Survey Open-File Report 2004-1042.

Quezada C R, Clement T P, Lee K, 2004. Generalized solution to multi-dimensional multi-species transport equations coupled with a first-order reaction network involving distinct retardation factors. Advances in Water Resources 27 (2004) 507–520 doi:10.1016/j.advwatres.2004.02.013

Randall J E, 2005. The analysis of seasonally varying flow in a crystalline rock watershed using an integrated surface water and groundwater model. Master Thesis, University of Waterloo, Waterloo, Ontario.

Rivett M O, Chapman S W, Allen-king R M, Feenstra S, Cherry J A, 2006. Pump-and-treat remediation of chlorinated solvent contamination at a controlled field-experiment site. Environmental Science & Technology, 40, 6770–6781.

Robinson C, Gibbes B, Li L, 2006. Driving mechanisms for groundwater flow and salt transport in a subterranean estuary. Geophys. Res. Lett., 33, L03402, doi:10.1029/2005GL025247.

Robinson C, Li L, Barry D A, 2007. Effect of tidal forcing on a subterranean estuary. Advances in Water Resources, 30: 851–865.

Rosenberry D O, Morin R H, 2004. Use of electromagnetic seepage meter to investigate temporal variability in lake seepage. Ground Water, 42(1): 68–77.

Savard C, Beaudoin G, Therrien R, 2007. Numerical modelling of 3D fluid flow and oxygen isotope exchange in fractured media: spatial distribution of isotope patterns. Geofluids, 7, 387–400.

Schmidt C, Bayer-Raich M, Schirmer M, 2006. Characterization of spatial heterogeneity of groundwater-stream water interactions using multiple depth streambed temperature measurements at the reach scale. Hydrology and Earth System Sciences, 10: 849–859.

Schuster P F et al. 2003. Characterization of lake water and ground water movement in the littoral zone of Williams Lake, a closed-basin lake in north central Minnesota. Hydrological Processes, 17: 823–838.

Shibuo Y, Jarsjö J, Destouni G, 2006. Bathymetry-topography effects on saltwater-fresh groundwater interactions around the shrinking Aral Sea. Water Resources Research, vol. 42, W11410, doi:10.1029/2005WR004207.

Sholkovitz E, Herbold C, Charette M, 2003. An automated dye-dilution based seepage meter for the time-series measurement of submarine groundwater discharge. Limnol. Oceanogr. Methods, 1: 16–28.

SKB, 2006. Model summary report for the safety assessment SR-Can. SKB TR-06-26, Svensk Kärnbränslehantering AB.

Smith L, Zawadzki W, 2003. A hydrological model of submarine groundwater discharge: Florida intercomparison experiment. Biogeochemistry, 66: 95–110.

Smith A J, 2004. Mixed convection and density-dependent seawater circulation in coastal aquifers. Water Resources Research, 40, W08309, doi:10.1029/2003WR002977.

Sohlenius G, Hedenström A, Rudmark L, 2004. Mapping of unconsolidated Quaternary deposits 2002–2003. Map description. Forsmark site investigation. SKB R-04-39, Svensk Kärnbränslehantering AB.

Sophocleous M, 2002. Interactions between groundwater and surface water: the state of the science. Hydrogeology Journal, 10(1): 52–67.

Sophocleous M, Perkins S P, 2000. Methodology and application of combined watershed and ground-water models in Kansas. Journal of Hydrology, 236: 185–201.

Swain E D, Wexler E J, 1996. A coupled surface-water and ground-water flow model (MODBRNCH) for simulation of stream–aquifer interaction. Techniques of Water-Resources Investigations, Book 6, Chapter A6, USGS.

Taniguchi M, 1993. Evaluation of vertical groundwater fluxes and thermal properties of aquifers based on transient temperature-depth profiles. Water Resour. Res., 29(7): 2021–2026.

Taniguchi M, Fukuo Y, 1993. Continuous measurements of ground-water seepage using an automatic seepage meter. Ground Water, 31: 675–679.

Taniguchi M, Fukuo Y, 1996. An effect of seiche on groundwater seepage rate into Lake Biwa. Water Resour. Res., 32: 333–338.

Taniguchi M, Iwakawa H, 2001. Measurements of submarine groundwater discharge rates by a continuous heat-type automated seepage meter in Osaka Bay, Japan. J. Groundwater Hydrol. 43: 271–277.

Taniguchi M, Burnett W C, Cable J E, Turner J V, 2002. Investigation of submarine groundwater discharge. Hydrological Processes, 16(11): 2115–2129.

Temnerud J, Bishop K, 2005. Spatial variation of streamwater chemistry in two Swedish boreal catchments: Implications for environmental assessment. Environmental Science & Technology, 39, 1463–1469.

Therrien R, McLaren R G, Sudicky E A, Panday S M, 2006. HydroGeoSphere. A Three-dimensional Numerical Model Describing Fully-integrated Subsurface and Surface Flow and Solute Transport. Groundwater Simulations Group. Draft, November 2006.

Tóth J A, 1962. A theory of groundwater motion in small drainage basins in Central Alberta, Canada. Journal of Geophysical Research, 67(11): 4375–4387.

Tóth J A, 1963. A theoretical analysis of groundwater flow in small drainage basins. Journal of Geophysical Research, 68(16): 4795–4812.

Turc L, 1954. The water balance of soils. Relation between precipitation, evaporation and flow. Annales Agronomiques 5, 491–569.

Van Deursen W P A, 1995. Geographical information systems and dynamic models; development and application of a prototype spatial modelling language. Ph.D. Thesis, Utrecht University, NGS Publication 190, 206 pp (Electronically available through www.carthago.nl).

Vanek V, Lee D R, 1991. Mapping submarine groundwater area-an example from Laholm Bay, southwest Sweden. Limnol. Oceanogr., 36(6): 1250–1262.

Voss C I, 1984. SUTRA. Saturated-unsaturated transport. A finite-element simulation model for saturated-unsaturated, fluid-density-dependent ground-water flow with energy transport or chemically-reactive single-species solute transport. U.S. Geol. Surv. Water Resour. Invest. Rep., 84–4369.

Wendland F, 1992. Die Nitratbelastung in den Grundwasserlandschaften der alten Bundesländer (BRD). Berichte aus der Okologischen Forschung, Band 8, Forschungszentrum Jülich, Jülich, 150pp.

Werner K, Bosson E, Berglund S, 2006a. Analysis of water flow paths: Methodology and example calculations for a potential geological repository in Sweden. Ambio, 35, 425–434 .

Werner K, Bosson E, Berglund S, 2006b. Description of climate, surface hydrology, and near-surface hydrogeology. Simpevarp 1.2. SKB R-05-04, Svensk Kärnbränslehantering AB.

Werner A D, Gallagher M R, Weeks S W, 2006c. Regional-scale, fully coupled modelling of stream-aquifer interaction in a tropical catchment. Journal of Hydrology, 328(3–4): 497–510.

Wiedemeier T H, Rifai H S, Wilson T J, Newell C, 1999. Natural Attenuation of Fuels and Chlorinated Solvents in the Subsurface, John Wiley, Hoboken, N. J.

Wilson A M, 2005. Fresh and saline groundwater discharge to the ocean: A regional perspective. Water Resources Research, 41, W02016, doi: 10.1029/2004WR003399.

Winter T C, Harvey J W, Franke O L, Alley W M, 1998. Groundwater and surface water – a single resource. U.S. Geol. Surv. Circular 1139.

Winter T C, 1999. Relation of streams, lakes, and wetlands to groundwater flow systems. Hydrogeology Journal, 7: 28–45.

Winter T C, Rosenberry D O, LaBaugh J W, 2003. Where does the ground water in small watersheds come from? Ground Water, 41(7): 989–1000.

Younger P L, 1996. Submarine groundwater discharge. Nature, 382, 121–122.

Zekster I S, 1996. Groundwater discharge into lakes: a review of recent studies with particular regard to large saline lakes in central Asia. International Journal of Salt Lake Research, 4: 233–249.

Appendix 1

Differences in lake properties used in the present PCRaster modelling and previous estimations by SKB

As was mentioned in the main text, the lakes in the present PCRaster model are significantly smaller than the ones in /Brunberg et al. 2004/. This is because the lakes in /Brunberg et al. 2004/ also include areas which are defined as wetlands in the PCRaster model (see Figure A1-1). As a result, the estimated mean depth and volume of the lakes also differ between /Brunberg et al. 2004/ and the present study, which is illustrated in Table A1-1. The estimated mean residence times differ between the two studies, not only because of the discrepancies in lake volume, but also due to different estimated mean discharge (see Table A1-2).

The reason for the large difference in estimated mean discharge for some lakes is probably that the area defined as the catchment of the lake is not the same in the two studies. Considering the flat topography in the Forsmark area, the characterisation of flow directions and sub-catchments is undoubtedly an exercise that is associated with large uncertainties.

Table A1-1. Comparison between the areas, mean depths and volumes of lakes estimated by /Brunberg et al. 2004/ and the same parameters estimated for the present PCRaster model.

Lake	Brunberg et al.			PCRaster model			$Area_{Br.}$ / $Area_{PCR}$
	Area (m^2)	Depth (m)	Volume (m^3)	Area (m^2)	Depth (m)	Volume (m^3)	
Gunnarsbo-Lillfjärden	56,255	0.54	29,980	31,900	0.84	26,800	1.8
Norra bassängen	76,070	0.31	23,650	42,200	0.44	18,700	1.8
Puttan	82,741	0.37	30,150	41,900	0.63	26,400	2.0
Bolundsfjärden	611,312	0.61	373,950	447,100	0.78	348,700	1.4
Labboträsket	60,042	0.27	15,950	15,100	0.63	95,00	4.0
Lake 2:2	9,921	0.29	2,861	6,600	0.36	2,400	1.5
Graven	50,087	0.12	5,920	16,800	0.16	2,700	3.0
Gunnarsboträsket	67,453	0.51	34,040	25,200	0.95	23,900	2.7
Tallsundet	79,414	0.23	18,350	23,900	0.53	12,700	3.3
Fräkengropen	19,423	0.19	3,660	5,500	0.42	2,300	3.5
Lake 4:1	35,058	0.38	13,000	9,300	0.86	8,000	3.1
Kungsträsket	7,733	0.2	1,550	3,000	0.36	1,100	2.6
Bredviken	97,664	0.74	72,010	68,400	0.99	67,700	1.4
Lillfjärden	161,269	0.29	47,030	74,600	0.51	38,000	2.2
Gällsboträsket	187,048	0.17	32,100	15,800	0.93	14,700	12
Lake 7:4	9,312	0.24	2,250	1,900	0.4	800	4.9
Vambörsfjärden	49,577	0.43	20,550	24,400	0.72	17,600	2.0
Märrbadet	23,611	0.36	8,500	11,000	0.6	6,600	2.1
Lake 7:3	6,393	0.25	1,620	2,100	0.45	900	3.0
Lake 7:1	163,052	0.32	52,570	110,400	0.4	44,200	1.5
Fiskarfjärden	754,303	0.37	274,450	419,600	0.55	230,800	1.8
Stocksjön	36,480	0.22	8,030	7,000	0.73	5,100	5.2
Eckarfjärden	283,850	0.91	257,340	221,500	1.12	248,100	1.3

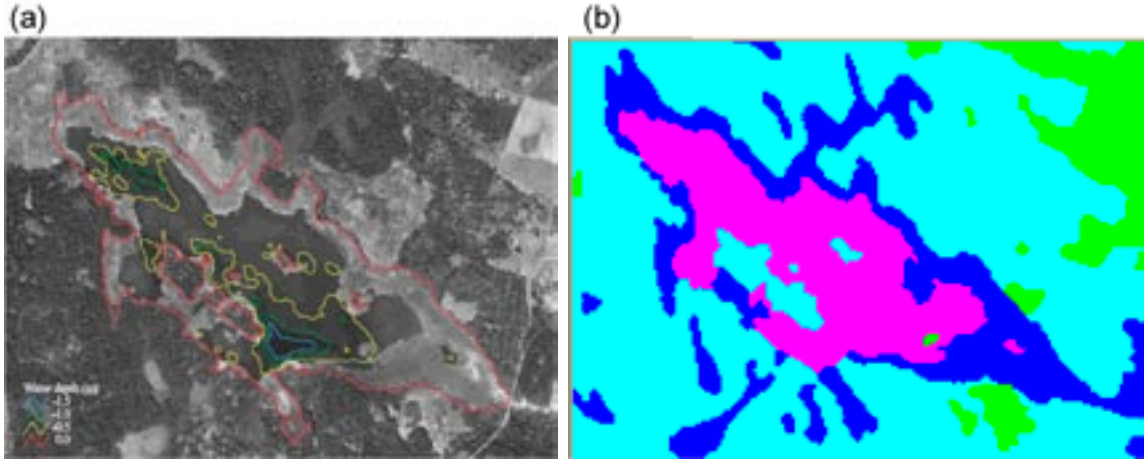

Figure A1-1. *The lake Fiskarfjärden according to (a) /Brunberg et al. 2004/ where the lake is defined as the area within the red line; and according to (b) the land use data on which the PCRaster model is based where the lake is represented by the pink areas and wetlands are represented by the blue areas.*

Table A1-2. Comparison between lake discharges and residence times estimated by /Brunberg et al. 2004/ and the same parameters estimated for the present PCRaster model.

Lake	Brunberg et al.		PCRaster model	
	Q (m^3/day)	Residence time (days)	Q (m^3/day)	Residence time (days)
Gunnarsbo-Lillfjärden	3,110	18	3,114	9
Norra bassängen	5,098	5	5,722	3
Puttan	5,270	6	121	218
Bolundsfjärden	4,838	77	5,408	64
Labboträsket	2,419	7	2,410	4
Lake 2:2	86	66	17	140
Graven	259	77	79	34
Gunnarsboträsket	1,642	21	1,900	13
Tallsundet	173	141	24	528
Fräkengropen	86	44	78	30
Lake 4:1	432	32	396	20
Kungsträsket	86	20	3	338
Bredviken	346	191	636	106
Lillfjärden	346	191	350	109
Gällsboträsket	1,728	18	712	21
Lake 7:4	86	49	1	1,276
Vambörsfjärden	259	70	52	338
Märrbadet	173	42	52	127
Lake 7:3	86	14	20	47
Lake 7:1	518	97	350	126
Fiskarfjärden	1,728	155	381	606
Stocksjön	1,123	9	56	91
Eckarfjärden	778	328	505	491

Appendix 2

Average delivery factors in different subareas for different transport scenarios

The first three rows in the table below show the delivery factors to the coast for the three considered transport scenarios. The fourth row shows the delivery factors to the surface water systems, the fifth row shows the delivery factors to the sea from the coastal catchments without surface water outflow, and the sixth row the delivery factors to the sea from the surface water systems.

	λ = 100/year	**λ = 10/year**	**λ = 1/year**	**λ = 0.1/year**	**λ = 0.01/year**	**λ = 0.001/year**
α_{gw} from the entire model area in scenario I	0.0063	0.031	0.13	0.52	0.92	0.99
α_{gw-s} from the entire model area in scenario II	0.02	0.075	0.38	0.86	0.98	1
α_{gw-s} from the entire model area in scenario III	0.012	0.051	0.25	0.69	0.95	1
α_{gw-s} upstream of surface water systems ($\gamma_{gw-s} = 1$)	0.00052	0.02	0.29	0.83	0.98	1
α_{gw-s} in coastal sub-catchments where $\gamma_{gw-s} = 0$	0.037	0.21	0.59	0.92	0.99	1
Delivery factor α_s from surface water systems to the sea	0.1	0.24	0.65	0.94	0.99	1

Appendix 3

Effects of travel time variability on total delivery factors

The table below shows the effects of travel time variability (V[lnT] = 1) on total delivery factors from the entire model area to the coast for different scenarios. The total/average delivery factors when the travel time variability is neglected are put in brackets for comparison.

	λ = 100/year	**λ = 10/year**	**λ = 1/year**	**λ = 0.1/year**	**λ = 0.01/year**	**λ = 0.001/year**
α_{gw} when V[lnT] = 1 in scenario I	0.011 (0.0063)	0.052 (0.031)	0.21 (0.13)	0.63 (0.52)	0.93 (0.92)	0.99 (0.99)
α_{gw-s} when V[lnT] = 1 in scenario II	0.031 (0.02)	0.14 (0.075)	0.5 (0.38)	0.87 (0.86)	0.98 (0.98)	1 (1)